UMEÅ UNIVERSITY

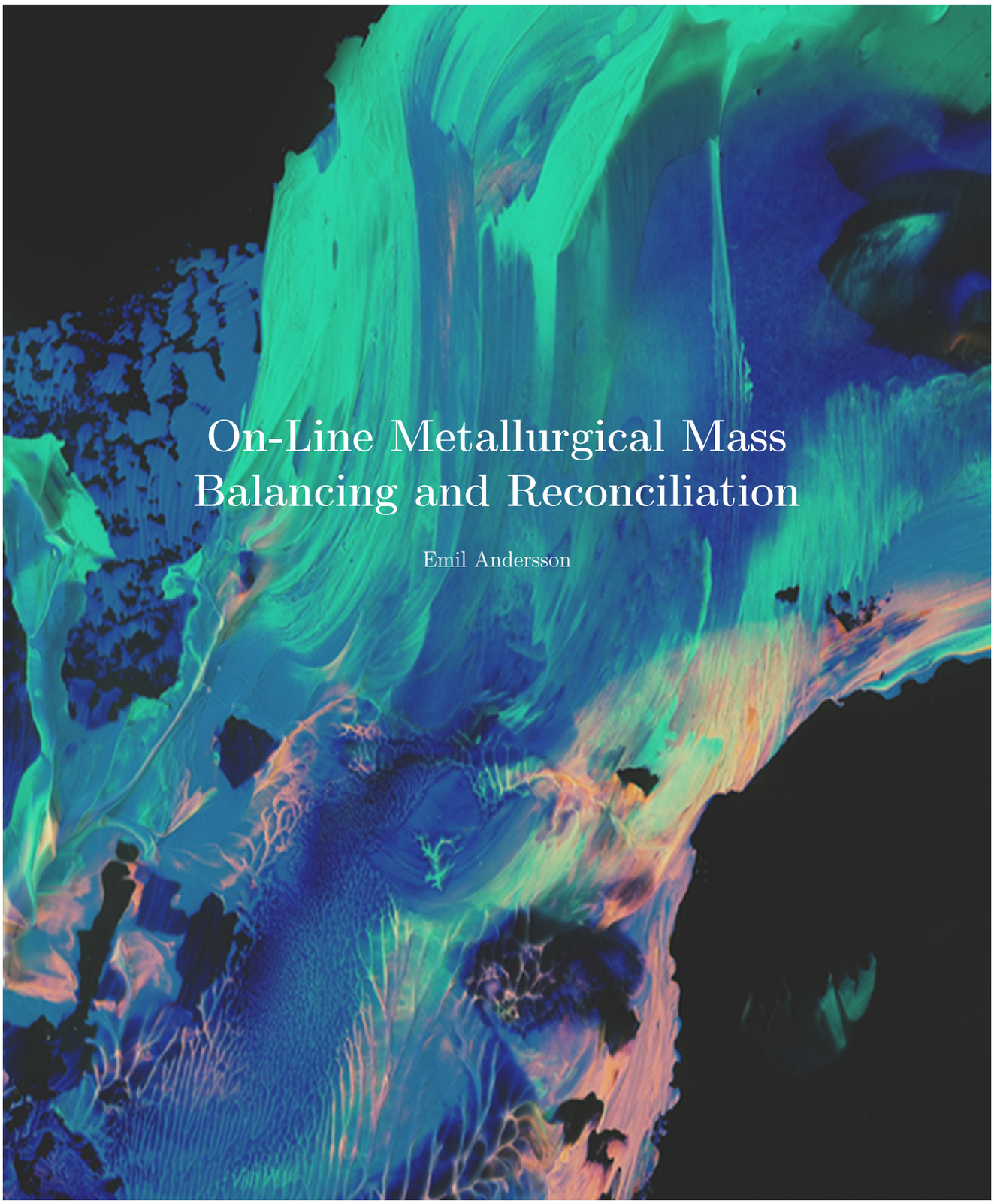

On-Line Metallurgical Mass Balancing and Reconciliation

Emil Andersson

Master thesis, 30 ECTS
Master of Science in Engineering Physics, 300 ECTS
Spring term 2021

On-Line Metallurgical Mass Balancing and Reconciliation

Author: **Emil Andersson**, emil960610@gmail.com
Supervisor: **David Degerfeldt**, Boliden AB, Skellefteå
Examiner: **Martin Berggren**, Dep. of Physics, Umeå University

Master Thesis in Engineering Physics, 30 ECTS
Department of Physics
Umeå University
SE-901 87 Umeå, Sweden

Abstract

In mineral processing, one of the most important and versatile separation methods is flotation. Flotation utilizes the different surface properties of the valuable minerals in the ore to separate them from the less valuable gangue material in the ore. Crushed and ground ore is mixed with water and fed into flotation tanks. In the flotation tanks, the particles of valuable mineral are made hydrophobic. That way, they can be floated by attaching to air bubbles and gather on top of the flotation tank as froth. This froth, containing higher concentrations of valuable mineral, is recovered and then processed further.

The flotation circuit is controlled and maintained using measurements on the mass flows and grades of different materials. Due to economical, practical, and technological limitations, these measurements are performed at a chosen number of points in the circuit and at discrete points in time. Poor measurement data can have devastating consequences if the operators are left with limited information and errors in the circuit remain undetected.

The accuracy of the acquired measurements is improved by performing mass balance and reconciliation. Traditionally, mass balance uses the sum of the total mass flows and the average grades over long times to avoid including the internal mass of the circuit in the calculations. It is desirable to perform mass balance directly to allow for faster intervention if any failures occur in the circuit during the on-line process.

This report describes an on-line dynamic approach towards mass balancing and reconciliation of the mass flows and grades in a flotation circuit. Here, physical models of the flotation circuit are used to construct mass balance constraints using interpolation and test functions and the mass balance problem is posed as an optimization problem. The optimization problem is to adjust the assay such that the residual, the difference between the measured and the adjusted assay, is minimized while maintaining mass balance.

An implementation in MATLAB and tests on synthetic data show that the dynamic formulation of mass balance does adjust 'erroneous' measurements such that mass balance is fulfilled. Given this result, there are still important aspects of the implementation that have to be addressed. The model uses the unknown and cell specific parameters flotation rate and recovery. Thus, these must be found or properly modeled. This report proposes a possible model for flotation rate as well as a strategy to find the recovery. The requirements of accuracy and speed of the implementation are also discussed.

Possible next steps of this project is to further confirm a time effective implementation using synthetic data. Consequently, the implementation can be adapted for natural data in order to verify correctness of models.

Sammanfattning

I malmanrikning, är flotation en av de viktigaste och mest mångsidiga metoderna. Flotation utnyttjar de fysikaliska ytegenskaperna som partiklar av värdemineral har för att separera dessa från det mindre värdefulla gråberget i malmen. Krossad och mald malm blandas med vatten och matas in i flotationstankar. I flotationstankarna görs partiklarna av värdemineral hydrofobiska. På så vis kan de fästa sig vid luftbubblor och flyta till ytan och bilda ett skum. Detta skum samlas sedan ihop och behandlas vidare eftersom det innehåller en högre koncentration av värdemineral.

Flotationskretsen styrs och underhålls med hjälp av mätningar av massflödena och halterna av de olika ämnena som finns i kretsen. På grund av ekonomiska, praktiska, och teknologiska hinder kan dessa mätningar bara göras på ett utvalt antal punkter i kretsen samt bara vid diskreta tillfällen. Felaktigt data kan ha förödande konsekvenser om operatörerna lämnas med begränsad information och processen fortlöper med oupptäckta fel.

Mätsäkerheten kan förbättras med hjälp av massbalansering och haltjustering. Traditionellt görs massbalansering genom att summera den totala massan som löpt genom kretsen samt medelvärden av halterna över lång tid för att undvika att räkna in den interna massan i systemet. Det är önskvärt att utföra massbalansering direkt för att möjliggöra snabbare ingrepp ifall fel uppstår i kretsen under den fortlöpande processen.

Denna rapport beskriver en dynamisk lösning för massbalansering och justering av massflöden och halter i en flotationskrets. Här används fysikaliska modeller av kretsen för att konstruera bivillkor för massbalans med hjälp utav interpolation och testfunktioner och massbalanseringsproblemet ställs upp som ett optimeringsproblem. Optimeringen sker genom att justera mätserien så att residualen, skillnaden mellan det uppmätta värdet och det justerade värdet, minimeras under uppfyllande av mass balans.

En implementation i MATLAB och tester på syntetisk data visar att den dynamiska formuleringen av massbalans justerar de felaktiga mätvärdena så att massbalans uppfylls. Med det resultatet i åtanke, finns det fortfarande viktiga aspekter av implementationen som bör tas hänsyn till. Modellen använder de okända och cellspecifika parametrarna flotationshastighet och utbytet och dessa måste kunna bestämmas för att denna modell ska kunna användas. Ett förslag på modellering av flotationshastigheten föreslås i rapporten. Dessutom ges förslag på strategier att hitta utbytet. Kraven på noggrannhet och snabbhet diskuteras också.

Möjliga nästa steg för projektet är att vidareutveckla en tidseffektiv implementation genom att använda syntetiska data. Därefter kan en implementation för naturligt data verifiera modellerna.

Contents

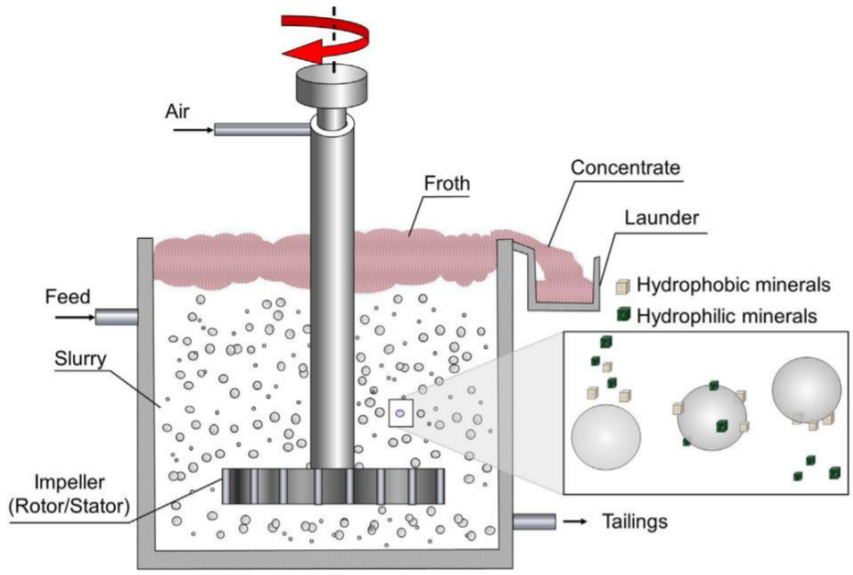

Figure 1: *Principles of froth flotation (Wills & Finch, Chapter 12: Froth Flotation, 2016) [1]*

1 Introduction

1.1 Background

The use of metals is ubiquitous in today's society. Metals are used to make the phones that we carry, the cars that we drive, the structures that we live in, and much more. The journey from mineral in the earth's crust to finished product is long, including prospecting, mining, refinement, and shipping. Through prospecting, metals is found in nature in its metallic form or as a composition of other materials depending on the reactivity of the metal. For example, gold and platinum are mainly found in their metallic state due to their low reactivity. Metals with high reactivity, like iron and beryllium, are predominately found in compounds such as oxides, sulfates, and silicates. Other metals, like silver and copper, are found both in their metallic form and in compounds. The compounds that are mined are referred to by the collective term *minerals*. The term mineral is also used in an business sense, defined by the value of the metals on the market. It is of great importance to have sufficient knowledge of minerals that one wants to mine [1].

The abundance of minerals across the earth differ due to geographical conditions. Deposits of greater concentration of minerals are called *ores*. Ores can be either metallic or non-metallic and the material in ores are split in two subgroups, *pay mineral* and *gangue*. The pay mineral is the valuable mineral in the ore while the gangue is the extraneous non-valuable material and the ore is mined in this composition [1].

After the ore has been mined, the ore has to be treated through *mineral processing*. This is the act of separating the pay mineral from the gangue. Mineral processing consists of two main parts, *liberation* and *concentration*. Liberation often refers to the act of crushing the ore into smaller particles, also called *comminution*, done by passing ore through mills. The aim is that each free particle should consist solely of one material. the subsequent step of concentration is the process through which the liberated particles of pay mineral and gangue are separated from each other. The aim is that as much as possible of the pay mineral is gathered in what is called the *concentrate* and that as much as possible of the gangue is gathered in what is called the *tailings*. There are multiple concentrating methods, and multiple physical properties of the mineral can be used for concentration, for example the density, the surface properties, and the electrical conductivity [1]. In this report, flotation is the main concentrating method that will be investigated. However, the theory is possible to extend to other processes.

1.2 Flotation

Froth flotation is a part of mineral processing that uses the surface property of the mineral in order to concentrate pay mineral, illustrated in figure 1. A mixture of water and comminuted ore, called *slurry* or *pulp*, is allowed to flow in to a flotation tank. The inflow is referred to as the *feed* of the tank. Reactants are added to the mixture in the flotation tank, for instance, to give the slurry the right PH-value, as well as making the particles with pay mineral hydrophobic and the particles with gangue material hydrophilic. Then, bubbles of air are introduced to large flotation tanks containing this mixture, and since the pay minerals are made hydrophobic they attach to these bubbles. The bubbles float to the top of the flotation tank, and the particles with pay mineral form a froth on the surface. The froth is allowed to run over the edge and is recovered in the launder on the side of the tank. The material is thereby split between two separate outflows, the *concentrate* and the *tail* [1]. To summarize, the purpose of the flotation process is to keep the grade of pay mineral in the concentrate as high as possible while minimizing the losses to tailings. A flotation plant is shown in figure 2.

A simplified standard flotation circuit is shown in figure 3. The masses that pass through the flotation circuit is measured at a finite number of chosen points in the system. The grades are measured using x-ray fluorescence analysis. However, due to economical and technological limitations the grades are sampled not continuously, but rather at discrete points in time. The most frequently updated sample point is updated roughly every fifteen minutes. The operators that control the flotation process depend heavily on this

Figure 2: *Flotation plant (Garpenberg, Boliden).*

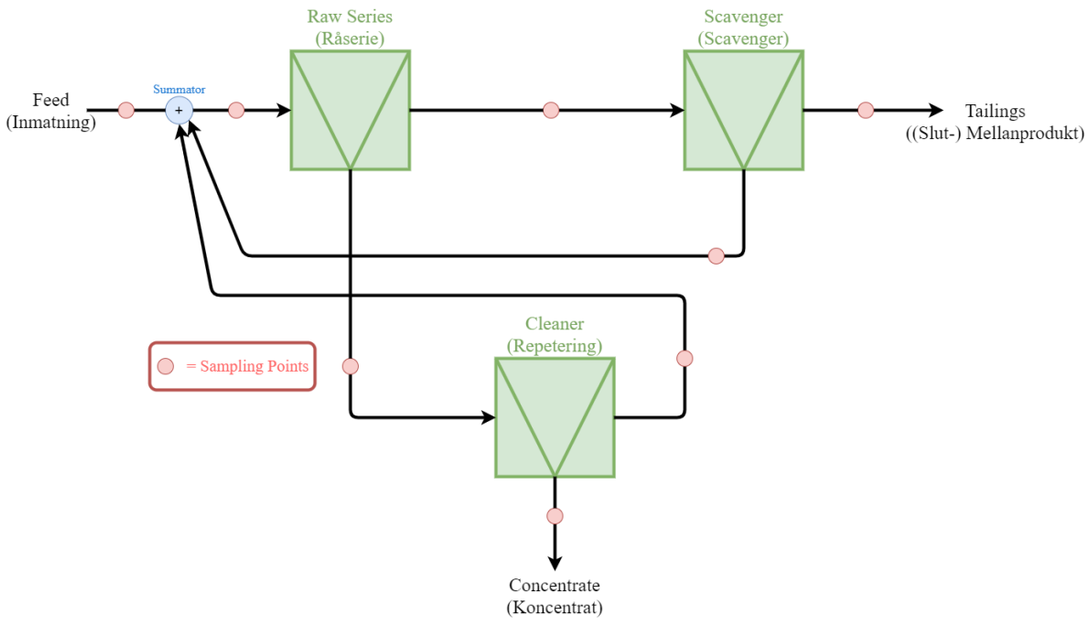

Figure 3: *A simplified typical flotation circuit. The circuit consists of three buffers named after where they are located in the circuit. The buffers consist of many flotation cells placed in series. The inflow to the circuit is called the feed and is where slurry of comminuted ore mixed with water is entered. The concentrate is where the slurry with high grade of pay mineral is transported, whereas the tailings is where the slurry of lower grade of pay mineral is transported. There are a limited number of measurement points in the circuit, marked with red circles.*

measured data because of the complex chemical processes involved in flotation. However, the data often suffers from poor quality [2], [3]. The measurements are done independently of each other and are done blindly, meaning that they do not take heed to any physical constraints. Furthermore, given that the conservation of mass can not be violated, the circuit must fulfill mass balance. Therefore, mass balance can be used to increase the measurement accuracy.

1.3 Notation

Before moving on, we introduce some notation. Here, circuits are simplified to flowcharts with buffers and products, as in figure 3. Products in the circuit refer to the flows between the buffers, i.e. inflows and outflows. These do only go in one direction, and no back flow occurs. Buffers refers to any point in the circuit where mass can build up, i.e. nodes in the circuit process mass over longer times. There are other types of buffers outside flotation cells, such as mills. The only other type of buffer considered in this report, other than flotation cells, are flotation *series* or banks. The residence time of a buffer depends on the nature of the buffer. Every buffer in this report is considered a flotation cell or series with one incoming product and two outgoing products, pictured in figure 4. Furthermore, a glossary is given in section A.

All calculations are performed on *dry* masses, meaning that the mass of the added water in the slurry is omitted from any calculation. The total dry mass flow includes the dry mass flow every material in the ore.

To be able to formulate mathematical expressions, many of quantities are needed. The quantities that are used in this report are listed in table 1.

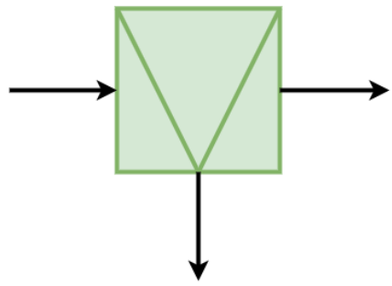

Figure 4: *Simple circuit displayed as a flow chart, one buffer with one incoming product and two outgoing.*

Table 1: *Notation table, showing the variables, their units, and the description of the quantities that occur in the report.*

Symbol	Unit	Description
t, τ	s	Time
$W_\alpha(t)$	kg	Total mass of element α in the node
$F(t)$	kg/s	Solid mass flow in the feed as a function of time t
$F_\alpha(t)$	kg/s	Mass flow of element α in the feed
$f_\alpha(t)$	-	The concentration of element α in the feed as a function of time t
$M(t)$	kg/s	Solid mass flow of metal in the tail/discharge stream as a function of time t
$M_\alpha(t)$	kg/s	Mass flow of element α in the tail/discharge stream
$m_\alpha(t)$	-	The concentration of element α in the tail/discharge stream as a function of time t
$C(t)$	kg/s	Solid mass flow in the concentrate stream as a function of time t
$C_\alpha(t)$	kg/s	Mass flow of element α in the concentrate stream
$c_\alpha(t)$	-	The concentration of element α in the concentrate stream as a function of time t
$R_\alpha(t)$	-	Recovery of material α from the feed to the concentrate
$\varphi_{\alpha,c}(t)$	1/s	Transfer function of element α from the feed to the concentrate
$\varphi_{\alpha,m}(t)$	1/s	Transfer function of element α from the feed to the tailings
$\phi_c(t)$	1/s	Residence time distribution of element α from the feed to the concentrate
$\phi_m(t)$	1/s	Residence time distribution of element α from the feed to the tailings
$\hat{x}$	-	Adjusted value of quantity x
$\tilde{x}$	-	Measured value of quantity x

1.4 Traditional Mass Balancing

The accuracy of the measurements done on flotation circuits can be improved by applying mass balance in the circuit. Traditional mass balancing is usually defined as an optimization problem; the residual is minimized by adjusting the assay such that mass balance is fulfilled. In other words, mass balance is the requirement for the adjusted values that are as close to the measured values as possible. The constraint of mass balance over a cell or sub-circuit ensures that the mass flow into the cell or sub-circuit is equal to the mass flow out of the same cell or sub-circuit. Done traditionally, one assumes steady state, sum the mass flows over time, and use assays that have been averaged over long time-periods. This way, all time-dependent delays that occur in the circuit can be neglected.

Here we consider only one flotation cell with feed, tail, and concentrate as shown in figure 5. The mass balance equations for this single cell are set up as a minimization problem: Find the values $\mathbf{x} = \{\hat{F}, \hat{f}_\alpha, \hat{M}, \hat{m}_\alpha, \hat{C}, \hat{c}_\alpha\}$ that minimize the objective function, the weighted residual

$$r(\mathbf{x}) = \sum_i^{N_i} \left(\frac{\tilde{x}_i - \hat{x}_i}{\sigma_i} \right)^2, \tag{1}$$

where σ_i is the expected measurement error of quantity x_i. The values $\mathbf{x}$ must fulfill the constraints

$$\begin{cases} \hat{F} - \hat{M} - \hat{C} = 0 \\ \hat{F}\hat{f}_\alpha - \hat{M}\hat{m}_\alpha - \hat{C}\hat{c}_\alpha = 0 \quad ,\forall\alpha. \end{cases} \tag{2}$$

The index α stands for element *alpha*. The adjusted values are bound by

$$\begin{cases} 0 \leq \hat{F}, \hat{M}, \hat{C} < \infty, \\ 0 \leq \hat{f}_\alpha, \hat{m}_\alpha, \hat{c}_\alpha \leq 1. \end{cases} \tag{3}$$

The expected error can be approximated using the standard deviation of the measurement. However, this does not take systematic errors into account.

The traditional method involves averaging over long times such that the internal mass that accumulates in the circuit does not contribute to the calculations. This approach can only effectively give retrospective information to increase the measurement accuracy, which is suitable for lab studies or totals done over long times. In an on-line process there exist buffers, or delays, in the circuit. For example, the flotation and milling processes are known buffers in the circuit. These delays cannot be neglected in an on-line approach and require modelling.

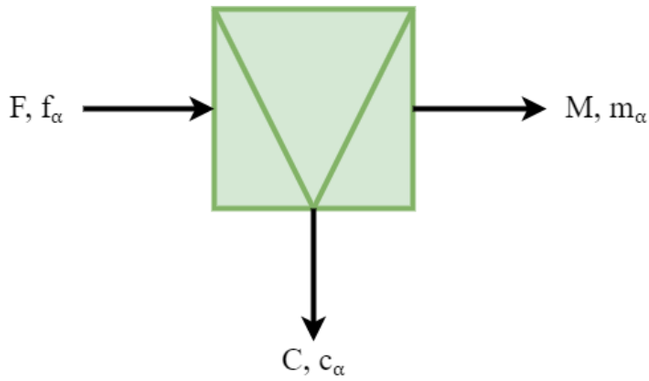

Figure 5: *A single flotation cell with one inflow and two outflows.*

1.5 Aim

It is important to understand that the flotation process is complex. It is an intricate circuit of pumps, machinery, sampling devices and more. It is crucial that all of these parts work together and that the process runs as continuously as possible. An undetected error can have devastating consequences. This is amplified by the marketable value of the material that passes through this circuit every hour of each day. Additionally, the flotation process is not an individual process, but rather it is only a small part of the mineral processing chain. The fact that flotation is a part of a long chain of processes means that other processes are affected as a consequence by poor performance in flotation.

A successful model would prove extremely valuable for mineral processing, since it enables the possibility for immediate response for the process operator. The access to accurate data of the metal grades in the process grants the possibility for immediate intervention of process failures so that the recovery of metal is maximized. This leads to both economical and ecological gain in saved energy cost and less pay mineral lost to tailings. Due to losses to tailings, there are tremendous losses in potential revenue annually. Just in the year of 2020, 3 000 ktonnes of ore were processed in Garpenberg to form metal concentrates of zinc, copper, lead, gold, and silver, with an operating profit of 1 942 MSEK [4]. If the concentrate grades of these metals all increased by one percent, it means means roughly 19 MSEK of profit for the year of 2020 alone for Garpenberg.

The solution to higher quality data is not necessarily more measurements. The grades are measured using a machine that performs x-ray fluorescence analysis on a representative sample of the slurry in a flow. Adding yet another machine would allow measurements to be performed more frequently. However, the data does still suffer from measurement errors, and mass balancing is still required to ensure quality of data. Additionally, the machine is in itself very complex, and there is personnel hired just for the maintenance and calibration of these. The addition of another machine would require more maintenance and would not significantly allow for better quality of data. The benefit of having another measuring device decreases for each additional machine that is already in use. Furthermore, empirical modelling is not an option since the tools must constantly be adjusted with the continuously changing processes and ore properties, there are inherent limitations of empiricism [3]. Therefore, improvements of the quality of data comes from a reliable formulation of on-line mass balancing.

The aim of this thesis work is to introduce a new mathematical formulation of on-line mass balancing and reconciliation of mass flows and grades in a flotation process. The idea is to start from the formulation of traditional mass balance and expand from there, gradually adding and developing physical models using interpolation and test functions to formulate time dependent constraints and goal function. The result can be used to to increase the quality of data from flotation circuits. After the optimization problem has been stated, verification can be performed using synthetic data of a simulated circuit. Finally, this report strives to make meaningful suggestions for future development of this project.

2 Theoretical Background

2.1 Recovery

When working with mass balancing of multiple outflows, it is useful to define the metal *recovery* R_α. This gives a measure of the amount of element α that was contained in the feed that can be found in the concentrate stream. This in turn is used as a measure of the metallurgical performance of a cell or sub-circuit. The recovery is given by [1]

$$R_\alpha = \frac{C_\alpha}{F_\alpha} = 1 - \frac{M_\alpha}{F_\alpha}. \tag{4}$$

2.2 Residence Time Distribution

The *residence time* of a fluid element is the total time the fluid element spends inside of a *control volume*, e.g. a flotation tank. The residence time for a set of fluid elements is referred to as a frequency distribution of the residence time of the set. This is known as the *Residence Time Distribution* (RTD), i.e. the mean residence time. The residence time is often of interest when working with continuously operating units and this transport behaviour is often determined by tracer tests. Tracer tests on liquids use the addition of some material such as salt, radioactive material, or coloring, that aids in measurement of the concentration in the inflow and the outflow and helps determining the time it takes for all of the material to pass through a control volume.

2.3 Convolution

Convolution is a mathematical operation that describes how two functions f and g form a third function $(f * g)$ that expresses how the shape of one function is modified by the other. The definition of convolution is

$$(f * g)(t) \coloneqq \int_{-\infty}^{\infty} f(\tau) g(t - \tau) d\tau, \tag{5}$$

and, since convolution is commutative,

$$(f * g)(t) \coloneqq \int_{-\infty}^{\infty} f(t - \tau) g(\tau) d\tau.$$

The function $f(t-\tau)$ is translated along the t-axis by τ. Therefore, the convolution $f * g$ can be thought of as a multiplication of translates of the function f. Since convolution is commutative, it is equally valid to consider $f * g = g * f$ as a multiplication of translates of g. Another way to interpret convolutions is as "moving weighted averages" [5].

2.4 Galerkin Approximations

A Galerkin approximation is a method used for approximating solutions to differential or integral equations. A solution is found by expanding it in a finite set of basis functions and projecting the equation on the same set of basis functions.

The so called weak formulation of an abstract problem is obtained by multiplying by a test function v and integrating over a suitable Hilbert space $\mathbb{V}$. The abstract weak formulation is thus

$$\text{find } u \in \mathbb{V} \text{ such that for all } v \in \mathbb{V},\ a(u, v) = f(v), \tag{6}$$

where $a(u, v)$ is a bilinear form and f is a bounded linear functional on $\mathbb{V}$.

A Galerkin approximation of (6) is obtained by choosing a subspace $\mathbb{V}_n \subset \mathbb{V}$ and solving the problem

$$\text{find } u_n \in \mathbb{V}_n \text{ such that for all } v_n \in \mathbb{V}_n, a(u_n, v_n) = f(v_n). \tag{7}$$

Since the vector subspace is finite-dimensional, a numerical solution to u_n can be found. The solution is found by numerically computing u_n as a finite linear combination of basis vectors in $\mathbb{V}_n$.

Galerkin approximations are the basis for Finite Element Methods. The idea is to rewrite differential equations in a weak form. The solution approximation can then be approximated using finite elements. This discretization results in a linear system that can be solved via computer [6].

2.5 Interpolation using Basis Functions

A common method to numerically approximate general functions is to use piecewise polynomials. The general idea is to approximate the actual function at a number of discrete points and use the piecewise polynomials to interpolate in space between the discrete points. In other words, these polynomials form a basis for the actual function and spans the space on which we want to interpolate. A continuous function $b(x)$ can thereby be approximated in terms of basis functions $\varphi_{b,i}(x)$ as

$$b(x) = \sum_{i=1}^{N_b} b_i \varphi_{b,i}(x), \tag{8}$$

where b_i is the amplitude of basis function $\varphi_{b,i}(x)$ and N_b is the number of basis functions used to describe $b(x)$ [6].

Continuous, piecewise linear polynomials are often used due to their simplicity. The standard basis functions for these fulfill the condition

$$\varphi_i(x_j) = \begin{cases} 1 & i = j, \\ 0 & i \neq j, \end{cases} \tag{9}$$

for sample points x_j. When these piecewise linear functions are extended over a continuous x domain they take on a triangular shape, which is why they are often referred to as hat functions. These hat functions are given by

$$\varphi_i(x) = \begin{cases} \frac{x - x_{i-1}}{x_i - x_{i-1}} & x_{i-1} < x < x_i, \\ \frac{x_{i+1} - x}{x_{i+1} - x_i} & x_i < x < x_{i-1}, \\ 0 & \text{otherwise}, \end{cases} \tag{10}$$

and these fulfill the condition given by equation (9) [6].

3 Method

3.1 First Formulation of On-Line Mass Balance

In on-line mass balancing, one has to work with mass flows rather than masses, i.e. $F \to F(t)$. Grades must also be allowed to change with respect to time, i.e. $f_x \to f_x(t)$, instead of being averaged over long times, see figure 6. Simply by inserting mass flows and time dependent grades into the traditional mass balance problem, described in section 1.4, we obtain a first formulation of on-line mass balance for a flotation node: Find the values $\mathbf{x} = \{\hat{F}, \hat{f}_\alpha, \hat{M}, \hat{m}_\alpha, \hat{C}, \hat{c}_\alpha, \}$ that minimize, the weighted residual

$$r(\mathbf{x}) = \sum_i^{N_x} \left(\frac{\tilde{x}_i - \hat{x}_i}{\sigma_i} \right)^2, \tag{11}$$

where σ_i is the expected measurement error of quantity x_i. The values $\mathbf{x}$ must fulfill the constraints

$$\begin{cases} F(t) - M(t) - C(t) = 0 \\ F(t)f_\alpha(t) + \frac{dW_\alpha(t)}{dt} - C(t)c_\alpha(t) - M(t)m_\alpha(t) = 0 \quad \forall \alpha. \end{cases} \tag{12}$$

The index α denotes element α. The values $\mathbf{x}$ must also satisfy the bounds

$$\begin{cases} 0 \leq \hat{F}(t), \hat{M}(t), \hat{C}(t) < \infty, \\ 0 \leq \hat{f}_\alpha(t), \hat{m}_\alpha(t), \hat{c}_\alpha(t) \leq 1. \end{cases} \tag{13}$$

Here, $W_\alpha(t)$ is the mass of metal α inside the flotation cell at time t.

The constraint for the total mass flow in equation (12) is similar to the constraints for the total masses in equation (2). This is due to the level sensor keeping the amount of mass in the node constant; the outflow of the node responds immediately to a change in inflow. It is important to note that this is a simplification. It is true that the volume of the tank remains constant; though it is not true for the *dry* mass in the cell. The composition of the comminuted ore that enters the node most definitely varies with time meaning that the mass in the node will change with time. This means that the total mass flow constraint would have a similar extra term as the grade mass flow constraint. However, this simplification is used in this report.

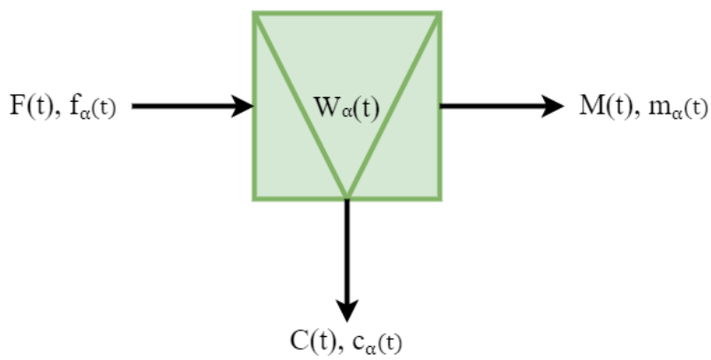

Figure 6: *A single flotation cell with one inflow and two outflows. The mass flow, grades, and internal mass vary with time.*

In contrast to the constraint for total mass, the updated constraint for the grades includes more than just an added time dependence. There is now the additional term $\frac{dW_\alpha(t)}{dt}$, see figure 6, in the constraint due to the fact that a change in grade in the feed is not immediately mediated to the concentrate and tail. Mass is allowed to accumulate and reside in the cell over a period in time, referred to as *residence time* in the node. Because of this residence time, the transfer of material through the node is delayed. Since the exact physics of the material transfer is very complicated to describe analytically, the material transfer in the nodes must be described using modelling.

3.2 Transfer Functions

To describe how the material is transferred through a node in a flotation circuit, transfer functions are modelled. The exact physics of time dependent buffers in a circuit, such as the mixing of material and reactants, is too complicated. These functions describe how the system respond to an impulse load. In this section the transfer functions for the tail and the concentrate are found, $\varphi_m(t)$ and $\varphi_c(t)$ respectively. This is done using flotation kinetics.

Techniques from signal processing are used to model the kinetics of the material in a flotation cell. Here the kinetics are simplified by assuming *plug flow*. Plug flow assumes that a mass W_0 is injected at time $t = 0$ and immediately evenly distributed in the cell, i.e. the material is perfectly mixed at injection. The flotation process in a cell is assumed analogous with calculations on chemical reactions. In this flotation "reaction" the reactants are the particle and bubble, and the product is the bubble-particle compound [1].

We consider a single cell that contains a constant volume. In the cell we assume that the reaction follows first order kinetics, that density of bubbles does not vary, and that a free particle can always "react with"

(attach to) an encountered bubble. Under these assumptions, the reduction in particle mass ($-dW/dt$) is proportionate to the mass in the cell (W). This is expressed as:

$$-\frac{dW(t)}{dt} = kW(t). \tag{14}$$

The constant k is a rate constant depending on the machine producing the bubbles, the particles in the pulp, and the froth; it is referred to as the flotation rate of the flotation cell. The higher the constant the higher the floatability [1]. More about this constant in section 3.6.

The simplest solution is found by assuming *batch flotation*, that is treating the particles as having the same residence time. By integrating from time 0 to t, we get the solution

$$W = W_0 e^{-kt}. \tag{15}$$

From this equation, the *Residence Time Distribution* (RTD) for the cell can be identified as

$$\phi(t) = e^{-kt}. \tag{16}$$

The RTD shows how the mass in the cell decays over time. The total outflow from the cell is thereby

$$-\frac{dW(t)}{dt} = W_0 k\phi(t) = W_0 k e^{-kt}. \tag{17}$$

Let's pause to consider an example of a system with similar exponential decay of material, illustrated in figure 7. There is a container with a hole in it and water is continuously being poured in to the container. For a steady state, the water level will remain the same since the inflow of water equals the outflow. Now imagine that at time $t = 0$ there is a mass of $W_{0,\mathrm{NaCl}}$ of salt evenly distributed in the container. The amount change in salt in the container will be related to the salt in the container at time t and can be described using equations (14) and (15).

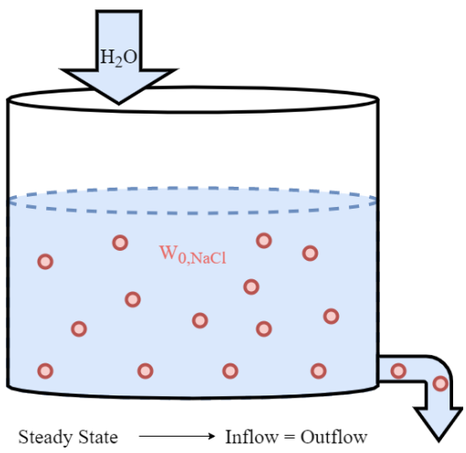

Figure 7: *A container of water. At time $t = 0$ the mass of salt in the container is $W_{0,NaCl}$. The amount of salt in the container decays exponentially.*

Now consider a flotation cell and the transfer of element α. The flotation cell has two outflows, the tail $M_\alpha(t)$ and the concentrate $C_\alpha(t)$. The recovery was defined in equation (4) to express the rate of discharge of element α through the concentrate. Thus, the recovery can be used here to distribute the material between the outflows. If it is assumed that the distribution is defined the exact moment when the material enters the cell, equation (17) becomes

$$M_\alpha(t) = \phi_m(t) W_{\alpha,0}(1 - R_{\alpha,t=0}), \tag{18}$$

$$C_\alpha(t) = \phi_c(t) W_{\alpha,0} R_{\alpha,t=0}. \tag{19}$$

Equations (18) and (19) can be extended to a continuous feed over time by convolution, as in section 2.3. Let the feed be $F(t)$, then

$$M_\alpha(t) = \int_{\tau=0}^{\infty} (1 - R_\alpha(t-\tau)) F_\alpha(t-\tau) \phi_m(\tau) d\tau, \tag{20}$$

$$C_\alpha(t) = \int_{\tau=0}^{\infty} R_\alpha(t-\tau) F_\alpha(t-\tau) \phi_c(\tau) d\tau. \tag{21}$$

Using these equations the transfer of material in a flotation cell can be calculated as long as we know the RTD. We can now replace the unknown term $\frac{dW(t)}{dt}$ in equation (12) and use the RTD to progress our model for on-line mass balancing. It is assumed that this expression can be used for each element α individually, i.e. that the transfer of one element is not affected by other elements.

Again, the RTD was found to be $\phi(t) = \phi_c(t) = \phi_m(t) = e^{-kt}$ for a single tank. In real flotation circuits, however, many tanks are positioned in series in order to extract pay mineral more efficiently. This effectively changes the transfer functions and consequently the RTD. These transfer functions for series are discussed further in section 3.5. Furthermore, it will be shown that the RTDs for the tail, $\phi_m(t)$, and concentrate, $\phi_c(t)$, are not the equal for a flotation series in contrast to the case of a single tank.

3.3 Second Formulation of Time Dependent Mass Balance

In the previous section, the transfer of material through a flotation cell was modeled and it was found that recovery of the cell and the RTDs of the concentrate and tail can be used to describe the transfer of material. Using this result, our previous formulation of the on-line mass balance problem can be extended. The optimization problem remains, with updated constraints and variables: Find the values $\mathbf{x} = \{\hat{F}(t), \hat{f}_\alpha(t), \hat{M}(t), \hat{m}_\alpha(t), \hat{C}(t), \hat{c}_\alpha(t)\}$ that minimize the weighted residual

$$r(\mathbf{x}) = \sum_i^{N_x} \left(\frac{\tilde{x}_i - \hat{x_i}}{\sigma_i} \right)^2, \tag{22}$$

where σ_i is the expected measurement error of quantity x_i. The values in $\mathbf{x}$ must fulfill the constraints

$$\begin{cases} F(t) - M(t) - C(t) = 0 \\ M(t)m_\alpha(t) - \int_0^\infty (1 - R_\alpha(t-\tau))\, F(t-\tau) f_\alpha(t-\tau)\phi_m(\tau)d\tau = 0 \\ C(t)c_\alpha(t) - \int_0^\infty R_\alpha(t-\tau) F(t-\tau) f_\alpha(t-\tau)\phi_c(\tau)d\tau = 0 \end{cases} \quad ,\forall\alpha. \tag{23}$$

The index α stands for element α and $\phi_m(\tau)$ is the RTD for the tailings and $\phi_m(\tau)$ is the RTD for the concentrate. The adjusted values are bound by

$$\begin{cases} 0 \leq \hat{F}(t), \hat{M}(t), \hat{C}(t) < \infty, \\ 0 \leq \hat{f}_\alpha(t), \hat{m}_\alpha(t), \hat{c}_\alpha(t) \leq 1. \end{cases} \tag{24}$$

Note that this is very similar to our previous formulation of mass balance, illustrated in figure 6. The objective function and the bounds remain identical. Even the mass balance constraint for the total mass flow remains the same. The only difference is that the second constraint has been divided into two new constraints, one for the tail and one for the concentrate. These constraints models the delay in material as it passes through the cell and relates portion of the inflow that is retained in each outflow.

However, the constraints for this formulation of mass balance are enforced for continuous time, both for the total mass flow constraints and the grade flow constraints. This means that there will be an infinite number of constraints, one for each point in time. Therefore, these constraints have to be appropriately discretized. In the following section, the constraints will be discretized such that a finite number of constraints can be enforced. This allows for a feasible real life implementation. Furthermore, the grades and mass flows are sampled at discrete points in time. Therefore, this information must be interpolated to all time. The discretization and interpolation are both done using techniques used in Finite Element Methods and will be done for both the total mass flow constraint and the grade flow constraints.

3.4 Discretization and Interpolation of the Constraints

The constraints must be discretized to be used in the formulation of mass balance in order to obtain a finite number of constraints. This is done, as described in section 2.4 using a Galerkin procedure, by multiplication of the constraints with a test function $\psi_j(t)$ and integrating the continuity equations for the tail and the concentrate over time:

$$\int_{-\infty}^{\infty} M(t)m_\alpha(t)\psi_j(t)dt = \int_{-\infty}^{\infty}\int_0^{\infty} (1 - R_\alpha(t-\tau))\, F(t-\tau) f_\alpha(t-\tau)\phi_m(\tau)\psi_j(t)d\tau dt \tag{25}$$

$$\int_{-\infty}^{\infty} C(t)c_\alpha(t)\psi_j(t)dt = \int_{-\infty}^{\infty}\int_0^{\infty} R_\alpha(t-\tau) F(t-\tau) f_\alpha(t-\tau)\phi_m(\tau)\psi_j(t)d\tau dt, \tag{26}$$

Where $j = 1, 2, ..., N_j$. This allows for selecting how many constraints one wants to enforce by choosing the test functions accordingly. These test functions can be choosen in a variety of ways.

Proceeding with these results we interpolate the mass flows and grades to find the values in between the sampling, approximating these as continuous functions. The interpolation is done, as described in section 2.5, using piecewise linear polynomials as basis functions, $\varphi_{x,i}$ where x is the quantity that is interpolated. The interpolation is done for the total mass flows as well as the grades in the feed, tail, and concentrate. E.g. interpolation gives the continuous equation for grade in the feed to be

$$f_\alpha(t) = \sum_{k=1}^{N_{f_\alpha}} f_{\alpha,k}\varphi_{f_{\alpha,k}}(t), \tag{27}$$

and the interpolation of the other grades and the mass flows are analogous.

Inserting the interpolated mass flows and grades into the discretized constraints in equation (25) gives

the expressions:

$$\int_{-\infty}^{\infty}\left(\sum_{i=1}^{N_M} M_i\varphi_{M_i}(t)\right)\left(\sum_{k=1}^{N_{m_\alpha}} m_{\alpha,k}\varphi_{m_{\alpha,k}}(t)\right)\psi_j(t)dt = \int_{-\infty}^{\infty}\int_{0}^{\infty}\left(1-\sum_{m=1}^{N_R} R_{\alpha,m}\varphi_{R,m}(t-\tau)\right)\left(\sum_{i=1}^{N_M} M_i\varphi_{M_i}(t-\tau)\right)\left(\sum_{k=1}^{N_{f_\alpha}} f_{\alpha,k}\varphi_{f_{\alpha,k}}(t-\tau)\right)\phi_m(\tau)\psi_j(t)d\tau dt, \tag{28}$$

$$\int_{-\infty}^{\infty}\left(\sum_{i=1}^{N_C} C_i\varphi_{C_i}(t)\right)\left(\sum_{k=1}^{N_{c_\alpha}} c_{\alpha,k}\varphi_{c_{\alpha,k}}(t)\right)\psi_j(t)dt = \int_{-\infty}^{\infty}\int_{0}^{\infty}\left(\sum_{m=1}^{N_R} R_{\alpha,m}\varphi_{R,m}(t-\tau)\right)\left(\sum_{i=1}^{N_M} F_i\varphi_{F_i}(t-\tau)\right)\left(\sum_{k=1}^{N_{f_\alpha}} f_{\alpha,k}\varphi_{f_{\alpha,k}}(t-\tau)\right)\phi_c(\tau)\psi_j(t)d\tau dt, \tag{29}$$

which are quite cumbersome. However, rearranging the terms in these expression gives

$$\int_{-\infty}^{\infty}\sum_{i=1}^{N_M}\sum_{k=1}^{N_{m_\alpha}} M_i\varphi_{M_i}(t)m_{\alpha,k}\varphi_{m_{\alpha,k}}(t))\psi_j(t)dt = \int_{-\infty}^{\infty}\int_{0}^{\infty}\sum_{m=1}^{N_R}\sum_{i=1}^{N_M}\sum_{k=1}^{N_{f_\alpha}}(1-R_{\alpha,m})\varphi_{R,m}(t-\tau)F_i\varphi_{F_i}(t-\tau)f_{\alpha,k}\varphi_{f_{\alpha,k}}(t-\tau))\phi_m(\tau)\psi_j(t)d\tau dt, \tag{30}$$

$$\int_{-\infty}^{\infty}\sum_{i=1}^{N_C}\sum_{k=1}^{N_{c_\alpha}} C_i\varphi_{C_i}(t)c_{\alpha,k}\varphi_{c_{\alpha,k}}(t))\psi_j(t)dt = \int_{-\infty}^{\infty}\int_{0}^{\infty}\sum_{m=1}^{N_R}\sum_{i=1}^{N_M}\sum_{k=1}^{N_{f_\alpha}} R_{\alpha,m}\varphi_{R,m}(t-\tau)F_i\varphi_{F_i}(t-\tau)f_{\alpha,k}\varphi_{f_{\alpha,k}}(t-\tau))\phi_c(\tau)\psi_j(t)d\tau dt. \tag{31}$$

Further, changing the order of summation and integration gives

$$\sum_{i=1}^{N_M}\sum_{k=1}^{N_{m_\alpha}} M_i m_{\alpha,k}\int_{-\infty}^{\infty}\varphi_{M_i}(t)\varphi_{m_{\alpha,k}}(t))\psi_j(t)dt = \sum_{m=1}^{N_R}\sum_{i=1}^{N_M}\sum_{k=1}^{N_{f_\alpha}}(1-R_{\alpha,m})F_i f_{\alpha,k}\int_{-\infty}^{\infty}\int_{0}^{\infty}\varphi_{R,m}(t-\tau)\varphi_{F_i}(t-\tau)\varphi_{f_{\alpha,k}}(t-\tau))\phi_m(\tau)\psi_j(t)d\tau dt, \tag{32}$$

$$\sum_{i=1}^{N_C}\sum_{k=1}^{N_{c_\alpha}} C_i c_{\alpha,k}\int_{-\infty}^{\infty}\varphi_{C_i}(t)\varphi_{c_{\alpha,k}}(t))\psi_j(t)dt = \sum_{m=1}^{N_R}\sum_{i=1}^{N_M}\sum_{k=1}^{N_{f_\alpha}} R_{\alpha,m}F_i f_{\alpha,k}\int_{-\infty}^{\infty}\int_{0}^{\infty}\varphi_{R,m}(t-\tau)\varphi_{F_i}(t-\tau)\varphi_{f_{\alpha,k}}(t-\tau))\phi_c(\tau)\psi_j(t)d\tau dt. \tag{33}$$

From the rearrangement it is easier to overview these new constraints and the final formulation of on-line mass balance can be made. Additionally, it can be noted here that the sampled values have been moved outside of the integral, leaving only "known" functions in the integrand.

So far, the focus in this section has been on the grade flows. However, there is is also need for discretizing and interpolating the total mass flow constraint. Therefore, similar operations are performed for the total mass flow. First, the total mass flow constraint in the constraint equations (23) is multiplied by the test function $\psi_j(t)$ and integrated over time

$$\int_{-\infty}^{\infty}\left(F(t)-M(t)-C(t)\right)\psi_j(t) = 0. \tag{34}$$

Then the same interpolation that was used for the mass flows of the grade constraints are used to give the linear constraints

$$\int_{-\infty}^{\infty}\left(\sum_{i=1}^{N_F} F_i\varphi_{F_i}(t)\psi_j(t) - \sum_{i=1}^{N_M} M_i\varphi_{M_i}(t)\psi_j(t) - \sum_{i=1}^{N_C} C_i\varphi_{C_i}(t)\psi_j(t)\right)dt = 0. \tag{35}$$

Changing the order of the integration and the summation gives the final expression for the total mass flow through a cell

$$\sum_{i=1}^{N_F} F_i\int_{-\infty}^{\infty}\varphi_{F_i}(t)\psi_j(t) - \sum_{i=1}^{N_M} M_i\int_{-\infty}^{\infty}\varphi_{M_i}(t)\psi_j(t) - \sum_{i=1}^{N_C} C_i\int_{-\infty}^{\infty}\varphi_{C_i}(t)\psi_j(t) = 0. \tag{36}$$

3.5 Transfer Functions for Series

In mineral processing plants where flotation is used, it is more common to make assays on series or blocks of tanks rather than individual tanks, considering these blocks as one step in the process. The behaviour of blocks is similar to that of individual flotation tanks, meaning that the same assumptions made when

modelling for individual tanks cells in section 3.2 can be made when modelling the transfer in a block. When modelling multiple flotation tanks in a series, there are some additional steps. The end products of this section are the expressions for the transfer functions to the tail and concentrate their respective RTDs. Initially, finding the RTDs comes from considering individual flotation tanks placed in a series, shown in figure 8, and adding the contribution of each. Note that the flotation tanks are connected such that the tail is the feed to the next tank in the series, and the concentrates of all the tanks in the series are combined to form a block concentrate stream.

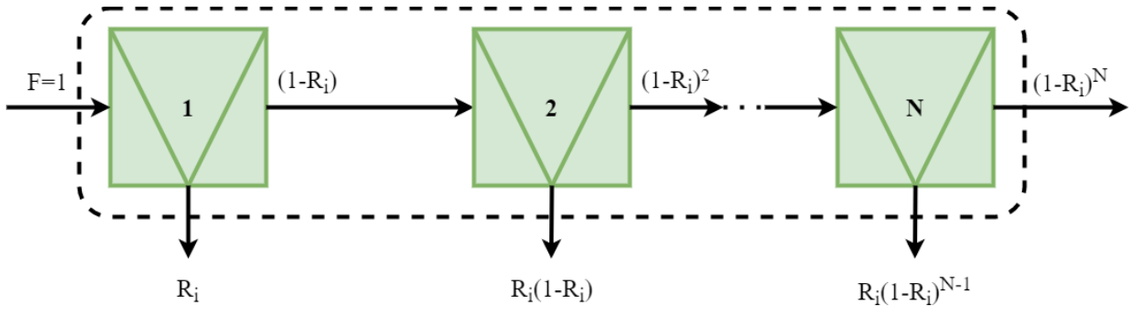

Figure 8: *Mass flows through a series of N flotation cells with equal cell recovery.*

3.5.1 Tail of Flotation Series

Assuming that every tank i in the series has the same recovery R_i, the change in mass in cell 2, given by W_2, equals the inflow minus the outflow. This is expressed by

$$\begin{aligned}\frac{dW_2}{dt} = M_1 - C_2 - M_2 = (1-R_i)kW_1 - R_ikW_2 - (1-R_i)kW_2 = \\ (1-R_i)kW_1 - kW_2 = (1-R_i)kW_0e^{-kt} - kW_2.\end{aligned} \tag{37}$$

Rewriting this expression gives

$$\frac{dW_2}{dt} + kW_2 = (1-R_i)kW_0e^{-kt}, \tag{38}$$

which is a standard Ordinary Differential Equation (ODE). With the boundary condition $W_2(0) = 0$, the solution to this ODE is

$$\begin{aligned}W_2(t) = e^{-kt}\left(\int e^{kt}(1-R_i)kW_0e^{-kt}dt + C\right) = e^{-kt}\left(\int (1-R_i)kW_0dt + C\right) = \\ e^{-kt}\left((1-R_i)kW_0t + C\right) = (1-R_i)ktW_0e^{-kt}\end{aligned}. \tag{39}$$

This can be repeated for tank 3 in the series

$$\begin{aligned}\frac{dW_3}{dt} = M_2 - C_3 - M_3 = (1-R_i)kW_2 - R_ikW_3 - (1-R_i)kW_3 = \\ (1-R_i)kW_2 - kW_3 = (1-R_i)k(1-R_i)ktW_0e^{-kt} - kW_3 = \\ (1-R_i)^2k^2tW_0e^{-kt} - kW_3,\end{aligned} \tag{40}$$

$$\frac{dW_3}{dt} + kW_3 = (1-R_i)^2k^2tW_0e^{-kt}, \tag{41}$$

$$\begin{aligned}W_3(t) = e^{-kt}\left(\int e^{kt}(1-R_i)^2k^2tW_0e^{-kt}dt + C\right) = \\ e^{-kt}\left(\int (1-R_i)^2k^2tW_0dt + C\right) = \\ e^{-kt}\left(\frac{1}{2}(1-R_i)^2k^2t^2W_0 + C\right),\end{aligned} \tag{42}$$

$$W_3(t) = \frac{1}{2}(1-R_i)^2(kt)^2W_0e^{-kt} \tag{43}$$

Similarly for tank 4 in the series the equations are found to be

$$\begin{aligned}\frac{dW_4}{dt} = M_3 - C_4 - M_4 = (1-R_i)kW_3 - R_ikW_4 - (1-R_i)kW_4 = \\ (1-R_i)kW_3 - kW_4 = (1-R_i)(1-R_i)^2(kt)^2W_0e^{-kt} - kW_4 = \\ \frac{1}{2}(1-R_i)^3k^3t^2W_0e^{-kt} - kW_4,\end{aligned} \tag{44}$$

$$\frac{dW_4}{dt} + kW_4 = (1-R_i)^3k^3t^2W_0e^{-kt}, \tag{45}$$

$$\begin{aligned}W_4(t) = e^{-kt}\left(\int e^{kt}(1-R_i)^3k^3t^2W_0e^{-kt}dt + C\right) = \\ e^{-kt}\left(\int (1-R_i)^3k^3t^2W_0dt + C\right) = \\ e^{-kt}\left(\frac{1}{6}(1-R_i)^3k^3t^3W_0 + C\right),\end{aligned} \tag{46}$$

$$W_4(t) = \frac{1}{6}(1-R_i)^3(kt)^3 W_0 e^{-kt} \tag{47}$$

By comparison of the above expressions, one can identify a generic behaviour. The generic expression for the mass in tank n in the series is

$$W_n(t) = \frac{1}{(n-1)!}(1-R_i)^{n-1}(kt)^{n-1} W_0 e^{-kt}. \tag{48}$$

The tail of the last tank in the series, tank N, is also the tail of the entire block. The tailings of this last tank is given by

$$\begin{aligned} M_N(t) = (1-R_i)kW_N(t) = (1-R_i)k\frac{1}{(N-1)!}(1-R_i)^{N-1}(kt)^{N-1}W_0e^{-kt} = \\ \frac{1}{(N-1)!}(1-R_i)^N k^N t^{N-1} W_0 e^{-kt}. \end{aligned} \tag{49}$$

From this, the transfer function can be identified by normalizing the tail flow against the amplitude of the impulse at t_0 i.e. multiplying the expression for the tail with $1/W_0$:

$$\varphi_{\alpha,m}(t) = \frac{M_N(t)}{W_0} = \frac{(1-R_i)^N}{(N-1)!}k^N t^{N-1} e^{-kt}. \tag{50}$$

The tail RTD of the block is found by normalizing the tail flow against the amplitude of the impulse W_0 and the tail recovery $1 - R_{\text{block}} = (1-R_i)^N$:

$$\phi_{m,N}(t) = \frac{M_N(t)}{W_0(1-R_i)^N} = \frac{1}{(N-1)!}k^N t^{N-1} e^{-kt}. \tag{51}$$

3.5.2 Concentrate of Flotation Series

To find the transfer function for the concentrate, one must sum the contributing concentrates from each tank, $C_n(t)$. To find the concentrate in each tank we reuse the expression we found for the mass in tank n, equation (48). Hence

$$C_n(t) = R_i k W_n(t) = \frac{1}{(n-1)!}R_i(1-R_i)^{n-1}k^n t^{n-1} W_0 e^{-kt} \tag{52}$$

This means that the expression for the concentrate of the entire block, $C_{\text{block}}(t)$, is given by

$$C_{\text{block}}(t) = \sum_{n=1}^{N} C_n(t) = \sum_{n=1}^{N} \frac{1}{(n-1)!}R_i(1-R_i)^{n-1}k^n t^{n-1} W_0 e^{-kt}, \tag{53}$$

from which the transfer function can be found by normalizing against the initial impulse

$$\varphi_{\alpha,c}(t) = \frac{C_{\text{block}}(t)}{W_0} = \sum_{n=1}^{N} \frac{1}{(n-1)!}R_i(1-R_i)^{n-1}k^n t^{n-1} e^{-kt}. \tag{54}$$

When all the tanks in the series have the same recovery, it is simple to find the recovery of the block from the mass balance of the block:

$$R_{\text{block}} = 1 - (1-R_i)^N. \tag{55}$$

Using the block recovery and the initial impulse amplitude W_0 to normalize the block concentrate flow, one can find the RTD of the block to be

$$\phi_{c,N}(t) = \frac{C_{\text{block}}(t)}{W_0 R_{\text{block}}} = \sum_{n=1}^{N} \frac{1}{(n-1)!}\frac{R_i(1-R_i)^{n-1}}{1-(1-R_i)^N}k^n t^{n-1} e^{-kt}. \tag{56}$$

3.6 Flotation Rate

When deriving the transfer functions in section 3.2, the flotation rate constant k was encountered. This constant is cell specific. The components of the cell that affect the rate constant k is the machine, the particles in the slurry, and the froth [1].

The machine is the source of production of bubbles. The amount of bubbles affects the bubble-particle reaction described in section 3.2. The machine factor has been related to the *bubble surface area flux* (BSAF) S_b. This is the rate of which the surface area of the bubbles moves through a cross-sectional area of the flotation cell, with the unit s^{-1}. As shown by Wills and Finch [1], BSAF can be approximated as

$$S_b = \frac{6J_g}{D_{32}} \tag{57}$$

where J_g [m/s] is the superficial gas velocity of the air in the bubbles and D_{32} [m] is the Sauter mean diameter of the bubbles. Both of these values are measurable using probes. The BSAF has been empirically shown to be proportional to the flotation rate constant in the pulp zone, such that

$$k_p = PS_b, \tag{58}$$

where P is a proportionality constant [1]. This new proportionality constant is some dimensionless quantity given that such both S_b and k_p have the unit s^{-1}. This constant reflects the particle properties, such as size, composition, and hydrophobicity, i.e. P is a measure of particle floatability. This applies to the slurry zone, but not the froth zone [1].

To find the flotation rate of the entire flotation cell, one must consider the fact that there is an interaction between the froth zone and the slurry zone of the flotation cell, i.e. there is the possibility of material in the froth zone to *drop back* to the slurry zone. To include the possible dropback interaction in calculations, the recovery of material from the froth zone R_f is defined. By definition, $(1 - R_f)$ is the dropback to the slurry zone. By performing mass balance calculations on the zones of a flotation cell that is fully mixed, the overall flotation rate of the cell can be expressed as [1]

$$k_{fc} = k_p R_f = P S_b R_f. \tag{59}$$

Techniques to quantify the froth recovery continue to be developed, though no method so far excels, as they are either intrusive or subject to assumptions [1]. Recently, a causal model for the froth recovery has been developed using the froth residence time, the froth volume, the volumetric froth flow rate, and the concentrate density [7].

4 Result

4.1 Final Formulation of On-Line Mass Balance

The constraints have been discretized to avoid an infinite number of constraints, and the samples have been interpolated to approximate continuous functions. This is combined with the model for transfer of mass through a flotation cell to formulate the optimization problem that gives on-line mass balance: Find the values $\mathbf{x} = \{\hat{F}_i, \hat{f}_{\alpha,k}, \hat{M}_i, \hat{m}_{\alpha,k}, \hat{C}_i, \hat{c}_{\alpha,k}\}$ that minimize the objective function, the weighted residual,

$$r(\mathbf{x}) = \sum_{i}^{N_x} \left(\frac{\tilde{x}_i - \hat{x}_i}{\sigma_i} \right)^2, \tag{60}$$

where σ_i is the expected measurement error of quantity x_i. The values in $\mathbf{x}$ must fulfill the constraints

$$\begin{cases} \sum_{i=1}^{N_F} \int_{-\infty}^{\infty} \varphi_{F_i}(t)\psi_j(t)dt F_i - \sum_{i=1}^{N_M} \int_{-\infty}^{\infty} \varphi_{M_i}(t)\psi_j(t)dt M_i - \sum_{i=1}^{N_C} \int_{-\infty}^{\infty} \varphi_{C_i}(t)\psi_j(t)dt C_i = 0, \\ \\ \displaystyle\sum_{m=1}^{N_R} \sum_{i=N_{F,t_0}}^{N_F} \sum_{k=N_{f_\alpha,t_0}}^{N_{f_\alpha}} A_{m,i,k}^{m,\alpha}(j)(1-R_{\alpha,m})\hat{F}_i\hat{f}_{\alpha,k} - \sum_{i=N_{M,t_0}}^{N_M} \sum_{k=N_{m_\alpha,t_0}}^{N_{m_\alpha}} B_{i,k}^{m,\alpha}(j)\hat{M}_i\hat{m}_{\alpha,k} = \\ - \left(\displaystyle\sum_{m=1}^{N_R} \sum_{i=1}^{N_{F,t_0-1}} \sum_{k=1}^{N_{f_\alpha,t_0-1}} A_{m,i,k}^{m,\alpha}(j)(1-R_{\alpha,m})\tilde{F}_i\tilde{f}_{\alpha,k} - \sum_{i=1}^{N_{M,t_0-1}} \sum_{k=1}^{N_{m_\alpha,t_0-1}} B_{i,k}^{m,\alpha}(j)\tilde{M}_i\tilde{m}_{\alpha,k} \right), \\ \\ \displaystyle\sum_{m=1}^{N_R} \sum_{i=N_{F,t_0}}^{N_F} \sum_{k=N_{f_\alpha,t_0}}^{N_{f_\alpha}} A_{m,i,k}^{c,\alpha}(j)R_{\alpha,m}\hat{F}_i\hat{f}_{\alpha,k} - \sum_{i=N_{C,t_0}}^{N_C} \sum_{k=N_{c_\alpha,t_0}}^{N_{c_\alpha}} B_{i,k}^{c,\alpha}(j)\hat{C}_i\hat{c}_{\alpha,k} = \\ - \left(\displaystyle\sum_{m=1}^{N_R} \sum_{i=1}^{N_{F,t_0-1}} \sum_{k=1}^{N_{f_\alpha,t_0-1}} A_{m,i,k}^{c,\alpha}(j)R_{\alpha,m}\tilde{F}_i\tilde{f}_{\alpha,k} - \sum_{i=1}^{N_{C,t_0-1}} \sum_{k=1}^{N_{c_\alpha,t_0-1}} B_{i,k}^{c,\alpha}(j)\tilde{C}_i\tilde{c}_{\alpha,k} \right), \\ \\ \forall \alpha. \end{cases} \tag{61}$$

where

$$A_{m,i,k}^{m,\alpha}(j) = \int_{-\infty}^{\infty} \int_{0}^{\infty} \varphi_{R,m}(t-\tau)\varphi_{F_i}(t-\tau)\varphi_{f_{\alpha,k}}(t-\tau)\phi_m(\tau)\psi_j(t)d\tau dt, \tag{62}$$

$$A_{m,i,k}^{c,\alpha}(j) = \int_{-\infty}^{\infty} \int_{0}^{\infty} \varphi_{R,m}(t-\tau)\varphi_{F_i}(t-\tau)\varphi_{f_{\alpha,k}}(t-\tau)\phi_c(\tau)\psi_j(t)d\tau dt, \tag{63}$$

and

$$B_{i,k}^{m,\alpha}(j) = \int_{-\infty}^{\infty} \varphi_{M_i}(t)\varphi_{m_{\alpha,k}}(t))\psi_j(t)dt, \tag{64}$$

$$B_{i,k}^{c,\alpha}(j) = \int_{-\infty}^{\infty} \varphi_{C_i}(t)\varphi_{c_{\alpha,k}}(t))\psi_j(t)dt. \tag{65}$$

The index α stands for element and $\phi_m(\tau)$ and $\phi_c(\tau)$ are the RTDs of material in the cell for the mass discharged via the tail and the concentrate respectively. The adjusted values are bound by

$$\begin{cases} 0 \leq \hat{F}_i, \hat{M}_i, \hat{C}_i < \infty, \\ 0 \leq \hat{f}_{\alpha,k}, \hat{m}_{\alpha,k}, \hat{c}_{\alpha,k} \leq 1. \end{cases} \tag{66}$$

This is the final formulation, which may be implemented for on-line mass balancing. Once again, note that this is the same constraints of previous formulations of the mass balance optimization problem, illustrated in figure 6. The difference from the second formulation in section 3.3 is that the constraints have been discretized and the sampled values have been interpolated to approximate using continuous functions. The discretization allows for the choice of number of constraints. One only has to choose the appropriate test functions, which can be chosen in a number of ways.

Note that the constraints on the left hand side are expressed in the adjustable degrees of freedom, $\hat{x}_i$, and on the right hand side are corresponding values, $\tilde{x}_i$, for times $t < t_0$. The right hand side are known historical values. Looking at the form of the RTDs, the discharge from the cell depends on previous samples in time to determine the present outflow. If there were only unknowns until the beginning of time then there could be no meaningful constraint set for the present. Thus, the constraint is truncated in time and fix historical samples are required in order to model the current continuous flow. These historical values are assumed to fulfill mass balance, and their expected relative error should be very small, close to zero.

Another complication that arises is that the recovery is required by this model. The recovery R_α is a cell specific parameter and is initially unknown and can change with time. The recovery can be calculated using equation (4). However, the recovery is found using the grade in the feed, concentrate and tail but these values are found using the recovery and so forth. Therefore, to find the recovery, the optimization can be reiterated. The idea is that the user submits an initial guess of what the recovery is $0 \leq R_0 \leq 1$. The mass balance is then performed using the submitted initial guess. After the mass balance has been performed, a new recovery can be computed from the balanced values with which the mass balance can be performed again. This can be repeated until the difference between the current and previous recovery is sufficiently small. This is a form of fixpoint iteration.

4.2 Residence Time Distribution of the Tail and Concentrate

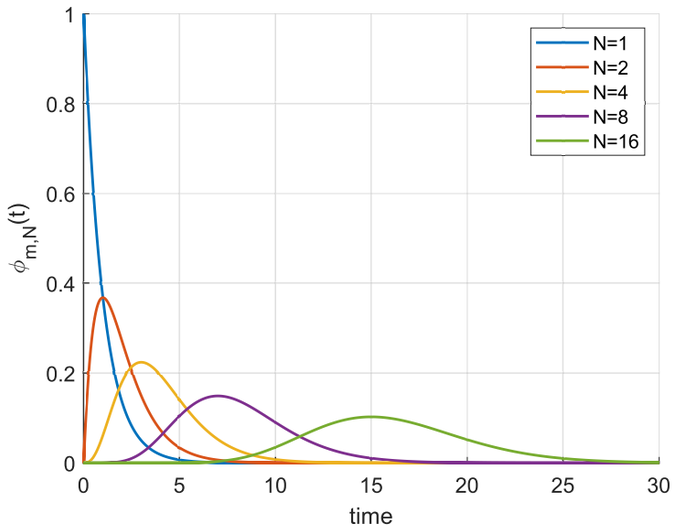

Figure 9: *Residence time distribution (RTD) for the last cell in a block with different number of cells, N. The block has flotation rate $k = 1.00$. The RTD has the same shape as the transfer function.*

The new dynamic formulation of mass balance for a flotation cell uses the RTD of the cell in the grade constraints. The RTDs for the material discharged through the tail and the concentrate have both been found as

$$\phi_{m,N}(t) = \frac{1}{(N-1)!} k^N t^{N-1} e^{-kt}, \tag{67}$$

$$\phi_{c,N}(t) = \sum_{n=1}^{N} \frac{1}{(n-1)!} \frac{R_i(1-R_i)^{n-1}}{1-(1-R_i)^N} k^n t^{n-1} e^{-kt}. \tag{68}$$

First, it is noted that the RTD for the tail does not depend on the recovery of the circuit. Another interesting thing to note is that

$$\int_0^\infty \phi_{m,N}(t)dt = \frac{k^N}{(N-1)!} \int_0^\infty t^{N-1} e^{-kt} dt = \frac{k^N}{(N-1)!} \frac{(N-1)!}{k^N} = 1. \tag{69}$$

Shown in figure 9 is the tail RTD for a couple of blocks with different N and $k = 1.00$.

In contrast to the tail, the RTD of the concentrate does vary with the recovery. This again poses a problem since the grades are needed to calculate the recovery, but the whole idea of of this model is to use the RTD to find the grades. This leaves us going in an endless loop. Hence, the recovery must be found some other way in order for this model to be used. The concentrate RTD is shown in figure 10 for a number of different block recoveries R_{block}. The block consist of $N = 16$ cells and the flotation rate $k = 1.00$. For high recoveries, the RTD tends towards exponential decay.

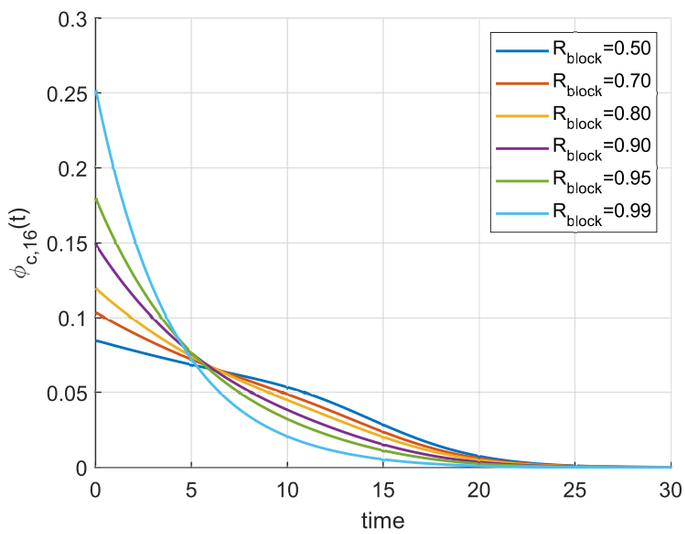

Figure 10: *Residence time distribution (RTD) for the concentrate of a series for different block recoveries $R_{block} = 1-(1-R_i)^N$, where R_i is the recovery for each individual cell. This has the same shape as the transfer function. The block has $N = 16$ cells and flotation rate $k = 1.00$.*

5 Verification

5.1 Structuring

The purpose of the formulated on-line mass balance is to find the grades and mass flows that fulfill the constraints and deviates as little as possible from the sampled quantities while also fulfilling the time dependent non-linear mass balance constraints set by the user. There exists optimization algorithms that can solve these kind of problems, handling both non-linear objective functions and constraints. It is merely a question of supplying the solver with the required values in the correct format. The program must be structured to handle the mass flows, grades, and buffers that exist in the circuit and insert the correct numbers into the correct equations.

The set up of the program is to represent the circuit by defined buffers in a circuit connected via products. One can think of buffers as nodes and products as one-way edges that connect the nodes. The purpose of this set up is to be able to tell for each buffer which products are connected to it and determine which of the products is the feed or discharge of the buffer. The samples of the connected products are then adjusted such that they fulfill mass balance for each test function ψ_j where $j = 1, 2, ..., N_j$. The number of constraints N_j is chosen by the user.

Rather than calculating and adjusting the values in the assay directly, the relative changes with respect to the assay are used as the degrees of freedom,

$$\mathbf{x} = \left\{ \frac{\hat{F}_i}{\tilde{F}_i}, \frac{\hat{f}_{\alpha,k}}{\tilde{f}_{\alpha,k}}, \frac{\hat{M}_i}{\tilde{M}_i}, \frac{\hat{m}_{\alpha,k}}{\tilde{m}_{\alpha,k}}, \frac{\hat{C}_i}{\tilde{C}_i}, \frac{\hat{c}_{\alpha,k}}{\tilde{c}_{\alpha,k}} \right\}. \tag{70}$$

This allows for an easier overview of the magnitude of adjustments. Using the relative changes also causes the adjustments of grades and mass flows to weigh equally in the residual. In other words, an adjustment by ten percent in a grade is considered to be of the equal magnitude as an adjustment by ten percent in a mass flow. This is important, since the mass flows are measured in the magnitude of tonnes while the grades are measured as numbers between zero and one. This means that all the calculations of the constraints and the objective function along with derivatives will have to take the vector (70) instead of the original vector.

In order to map every degree of freedom to its respective value in the circuit, a *mass2dof*-vector and *grade2dof*-matrix are used. The mass2dof-vector is a $(N_{\text{samples}}, 1)$ vector and contains the index of the adjustable value in $\mathbf{x}$. If the value is not adjustable, but rather a fix historical value, then the value for that index is -1. The grades2dof-matrix is implemented in a similar way but has the size $(N_{\text{samples}}, N_{\text{elements}})$. These mapping tools are used in the implementation in order to distinguish the degrees of freedom and fix values from each other as well as retrieve the correct degree of freedom for the correct equations.

The optimization problem was implemented using MATLAB. To allow for versatility in the code, the products, buffers, circuits, topology of the circuits, and mass balancing problems were each assigned as classes [8]. A class can be thought of as a blueprint for objects that each have assigned properties and functions. This way, these parts of the problem could be handled as objects. This allows for easier construction of the system and handling of data.

5.2 Classes and Responsibilities

Buffer - A buffer is a node in the circuit where mass can accumulate. It is the responsibility of the buffer to know its recovery, flotation rate k, and its RTD for both the tail and the concentrate. The RTDs depend on the number of flotations tanks that are in the series according to equations (68) and (67). The buffer must therefore know the number N cells in the series.
Product - A product is a one-way flow in the circuit. It is in the products that the grades and mass flows are measured. The responsibility of the product class is to know the time stamp and values each time the grade and the mass flows were measured. The product does also know the expected absolute and relative error of the measurements, which also tells which measurement is fixed and historical, and which measurement is a degree of freedom.
Topology - The topology class is used to map the buffers and products. It holds the connectivity matrix of the circuit, size $\mathbb{R}^{(N_{\text{buffers}} \times N_{\text{products}})}$. Rows in the connectivity circuit represents the buffers in the circuit while the columns represent the products. The elements in the connectivity circuit are 1 for products that terminate in the buffer and -1 for products that originate from a buffer and 0 otherwise. Logically, a product can only originate from one buffer and terminate in one buffer.
Assay - The assay class holds all the buffers, products in the circuit as well as the topology of the circuit. In a way, it can be thought of as the circuit with all the measurements. The purpose of this class is to allow easy access to any of the products and buffers in the circuit using the connectivity matrix. It is also the assays responsibility to create the mass2dof-vector and grades2dof-matrix.
TimeDepMassBalance - This class holds the optimization problem. The class for time dependent mass balancing holds one assay and performs the mass balance described in this report for all the buffers and products in the circuit by creating the corresponding constraints, objective function and bounds. In this implementation, MATLAB's built-in optimizer `fmincon` was used.

5.3 Numerical Optimization

To solve the optimization problem, MATLAB's built-in function `fmincon` was used [9]. This function minimizes an objective function and handles constraints, both linear and nonlinear. The function finds the

minimum of the problem specified by

$$\min_x f(x) \text{ such that } \begin{cases} c(x) \leq 0 \\ ceq(x) = 0 \\ A \cdot x \leq b \\ Aeq \cdot x = beq \\ lb \leq x \leq ub, \end{cases} \tag{71}$$

where b and beq are vectors, A and Aeq are matrices, $c(x)$ and $ceq(x)$ are functions that return vectors, and $f(x)$ is a function that returns a scalar. The functions $f(x)$, $c(x)$, and $ceq(x)$ are allowed to be nonlinear functions. All constraints linear and nonlinear are separated between equality or inequality constraints.

In the optimization problem for the on-line mass balance, the objective function $f(x)$ is the residual $r(\mathbf{x})$ given by (60). The total mass flow constraint in (61) is a linear equality constraint and the grade flow constraints in (61) are non-linear equality constraints.

The function `fmincon` contains a number of algorithms for optimization. The default, which is also used in this report, is the *'interior-point'* algorithm. The approach of this algorithm is to solve a number of approximate minimization problems [10]. This algorithm handles large sparse problems as well as small dense problems and it handles bounds at all iterations. The algorithm uses the gradient of the objective function and the gradient and the Hessian of the non-linear constraints to determine the steps taken by the solver. If there are no supplied gradients nor Hessian then the algorithm uses finite differences to approximate these.

To supply the Hessian to the algorithm, the matrix of second order derivatives of the Lagrangian $L(x, \lambda)$ must be supplied [9]:

$$\nabla^2_{xx} L(x, \lambda) = \nabla^2 f(x) + \sum \lambda_i \nabla^2 c_i(x) + \sum \lambda_i \nabla^2 ceq_i(x). \tag{72}$$

Here x is the input vector $\mathbf{x}$ with the adjustable values. The Hessian will be a symmetric matrix with the size $(N_{DoF} \times N_{DoF})$, where N_{DoF} is the number of adjustable variables.

The optimization function requires an initial point $\mathbf{x}_0$ to carry out the minimization. A natural initial point to use is the initial assay values $\tilde{x}$. This is equivalent to $x_{0,i} = \frac{\hat{x}}{\tilde{x}} = 1, \forall i$.

5.4 Implementation

5.4.1 The objective Function and Bounds

The objective function was straight-forward to implement. In this implementation, the degrees of freedom are submitted as the fraction of the adjusted value and the measured value, $\frac{\hat{x}_i}{\tilde{x}_i}$

$$f(x) = r(\mathbf{x}) = \sum_{i=1}^{N_{DoF}} \left(\frac{\frac{\hat{x}_i}{\tilde{x}_i} - 1}{\sigma_i} \right)^2. \tag{73}$$

Here $\hat{x}_i$ is the ith adjustable degree of freedom, $\tilde{x}_i$ is the sampled value corresponding to the degree of freedom, and σ_i is the expected measurement error of the sampled value.

The optimization function `fmincon` uses the gradient of the objective function to determine the step size. If the gradient of the objective function is not supplied then the function uses finite differences to compute the approximate gradient. The gradient of the objective function, $\nabla_{\hat{x}_i} r(\mathbf{x})$ is quite simple to evaluate analytically since there are no cross products every element i only contains terms of $\hat{x}_i$. If it is supplied to `fmincon` it saves computational time of the mass balancing. The analytical gradient is given by

$$\nabla_{\hat{x}_i} r(\mathbf{x}) = \frac{2}{\sigma^2} \left(\frac{\hat{x}_i}{\tilde{x}_i} - 1 \right) \tag{74}$$

The bounds are also very intuitive to implement. The vector for lower bounds is simply $lb = \mathbf{0}$ while for every mass the upper bound $ub_{\text{mass}} = \infty$ and for every grade the upper bound is set to $ub_{\text{grade}} = 1$

5.4.2 Linear Constraints

The optimization function `fmincon` requires the linear constraints to be supplied on the form $A\mathbf{x} = \mathbf{b}$, as in (71). The constraint of the total mass flow in equation (61) form the linear constraint

$$\sum_{i=1}^{N_F} F_i \int_{-\infty}^{\infty} \varphi_{F_i}(t)\psi_j(t) - \sum_{i=1}^{N_M} M_i \int_{-\infty}^{\infty} \varphi_{M_i}(t)\psi_j(t) - \sum_{i=1}^{N_C} C_i \int_{-\infty}^{\infty} \varphi_{C_i}(t)\psi_j(t) = 0. \tag{75}$$

There are only known functions inside of the integral. Each row in the matrix $Aeq \in \mathbb{R}^{(N_j \times N_{DoF})}$ will contain the correspond to the constraint set by test function $\psi_j(t)$ and each column correspond to the degree of freedom $\hat{x}_i$, where $i = 1, 2, ..., N_{DoF}$. Obviously, the grades are not considered in this constraint. Thus, $Aeq = 0$ for each element in Aeq that correspond to a grade. For each element that correspond to a mass degree of freedom, the element is

$$Aeq_{i,j} = \begin{cases} +\int_{-\infty}^{\infty} \varphi_i(t)\psi_j(t)dt & \text{if product is feed,} \\ -\int_{-\infty}^{\infty} \varphi_i(t)\psi_j(t)dt & \text{if product is outflow,} \\ 0 & \text{otherwise.} \end{cases} \tag{76}$$

Somewhat similar for the vector $beq \in \mathbb{R}^{(N_j \times 1)}$, all fix historical mass flows F_i, M_i, and C_i of the connected products create the right hand side by

$$beq_j = -\left(\sum_{i=1}^{N_F} F_i \int_{-\infty}^{\infty} \varphi_{F_i}(t)\psi_j(t) - \sum_{i=1}^{N_M} M_i \int_{-\infty}^{\infty} \varphi_{M_i}(t)\psi_j(t) - \sum_{i=1}^{N_C} C_i \int_{-\infty}^{\infty} \varphi_{C_i}(t)\psi_j(t)\right). \tag{77}$$

All integrals are computed using MATLAB's built-in function `integral` [11].

5.4.3 Non-Linear Constraints

The grade constraints in equation (61) are non-linear since they contain the product mass flows and grades. The function `fmincon` requires the input of a function that returns the two arrays c and ceq. Every element of both of the arrays should contain an equality or an inequality constraint Since there are no non-linear inequality constraints, our non-linear constraint function should return $c = [\ ]$. On the other hand, the non-linear constraint function computes the constraints for every buffer and every test function $\psi_j(t)$ as well as for every material α. For every test function $\psi_j(t)$, for every buffer in the circuit, and for every element α, there are two grade constraint equations, the constraints formulated in (61). Double integrals are computed using the MATLAB function for numerical double integration, `integral2` [12]:

$$\begin{aligned}\sum_{m=1}^{N_R}\sum_{i=1}^{N_M}\sum_{k=1}^{N_{f_\alpha}}(1-R_{\alpha,m})F_i f_{\alpha,k}\int_{-\infty}^{\infty}\int_{0}^{\infty}\varphi_{R,m}(t-\tau)\varphi_{F_i}(t-\tau)\varphi_{f_{\alpha,k}}(t-\tau))\phi_m(\tau)\psi_j(t)d\tau dt- \\ \sum_{i=1}^{N_M}\sum_{k=1}^{N_{m_\alpha}} M_i m_{\alpha,k}\int_{-\infty}^{\infty}\varphi_{M_i}(t)\varphi_{m_{\alpha,k}}(t))\psi_j(t)dt = 0,\end{aligned} \tag{78}$$

$$\begin{aligned}\sum_{m=1}^{N_R}\sum_{i=1}^{N_M}\sum_{k=1}^{N_{f_\alpha}}R_{\alpha,m}F_i f_{\alpha,k}\int_{-\infty}^{\infty}\int_{0}^{\infty}\varphi_{R,m}(t-\tau)\varphi_{F_i}(t-\tau)\varphi_{f_{\alpha,k}}(t-\tau))\phi_c(\tau)\psi_j(t)d\tau dt- \\ \sum_{i=1}^{N_C}\sum_{k=1}^{N_{c_\alpha}} C_i c_{\alpha,k}\int_{-\infty}^{\infty}\varphi_{C_i}(t)\varphi_{c_{\alpha,k}}(t))\psi_j(t)dt = 0.\end{aligned} \tag{79}$$

5.4.4 Test Functions

The test functions allow for choice of number of enforced constraints. The constraints should be enforced in time such that all of the adjustable values are involved in the evaluation of the constraints. In this implementation, the constraints are constructed using the test functions

$$\psi_j(t) = \varphi_j(t) = \begin{cases} \frac{t-t_{j-1}}{t_j-t_{j-1}} & t_{j-1} < t < t_j \\ , \frac{t_{j+1}-t}{t_{j+1}-t_j} & t_j < t < t_{j-1} \\ , 0 & \text{otherwise.} \end{cases} \tag{80}$$

These are hat functions described in section 2.5. The times $t_j, j = 1, 2, ..., N_j$, are chosen such that t_1 is the sample time of the first chronological adjustable degree of freedom and t_{N_j} is the sample time of the sample time of the last chronological adjustable degree of freedom. In the end, N_j number of points in time are chosen, equally distanced from each other. The user specifies the number of constraints N_j that are to be implemented. More implemented test functions means more enforced constraints, but this also increases the number of numerical operations required. Thus, one must consider the required accuracy with respect to the computational speed.

5.5 Single-Cell Tests

In these tests, a single cell has been simulated. The system consists of two buffers, one being the flotation cell and the other being the 'outside'. The outside buffer is needed since products need a source and a destination. If there was no outside buffer, then the only possible set up would be a closed loop. The number of tanks in the buffer can be set to any positive integer. This changes the RTDs for both the tail and the concentrate according to equations (67) and (68).

There are three products in the system: the feed, the tail, and the concentrate. All of these have eight samples, all measured at times $t_i = 0, 10, ..., 70$. All products have sampled mass flows and sampled grades for two elements, simply called element1 and element2. There is a constant mass flow throughout the system, the feed $F_(t_i) = 100$, the tail $M(t_i) = 80$, and the concentrate $C(t_i) = 20$. In these mass flows the grades of element1 and element2 are constant, the grades in the feed $f_1(t_i) = f_2(t_i) = 0.2$, the grades in the tail $m_1(t_i) = m_2(t_i) = 0.1$, and the grades in the concentrate $c_1(t_i) = c_2(t_i) = 0.6$. With cell recovery set to $R_1 = R_2 = 0.6$, this assay of constant flows and grades fulfills mass balance.

Here all adjustable degrees of freedom are given the expected error $\sigma_i = 0.1$ meaning that there is an expected measurement error of 10%. This involves all sampled values except for the values sampled at times $t_1 = 0$, $t_2 = 10$, and $t_3 = 20$. These samples are chosen as the "accepted history" of the assay. These samples have an expected error of $\sigma_i = 0$ meaning that they are considered confirmed as the true values.

5.5.1 Optimization on Assay That Fulfills Mass Balance

Given that the initial system fulfills mass balance, the implementation should not stray from this solution by adjusting any values in the assay. The implementation should also adjust the values to be equal to the initial assay, if the initial point $\mathbf{x_0}$ is taken to be not equal to the initial assay.

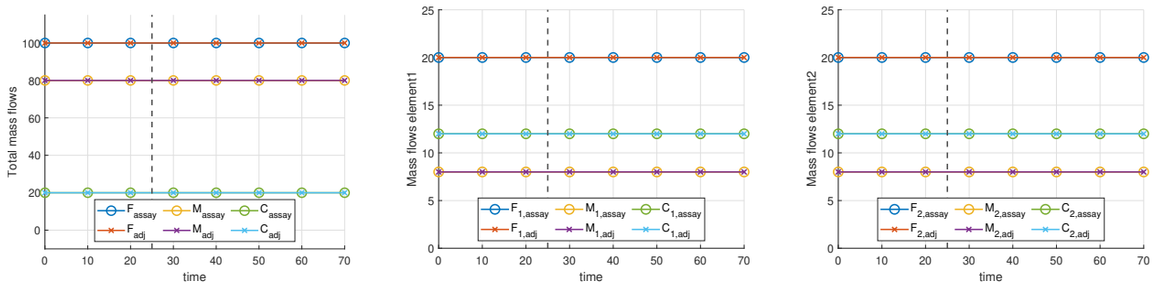

(a) Total mass flow (b) Mass flow element1 (c) Mass flow element2

Figure 11: *Assay and the adjusted values. The values to the left of the dashed lines are fixed while the values to the right are adjustable. The initial assay fulfill mass balance and there are no adjustments needed.*

The optimization was performed using the initial assay as the initial point. As expected, the result show that the initial point minimizes the objective function within the constraints. The plotted samples are shown in the figure 11.

Furthermore, the optimization yielded the same results using the initial point is taken as 0.5 of the assay samples, shown in figure 12. Therefore, the solution of the implementation is assumed to be stable.

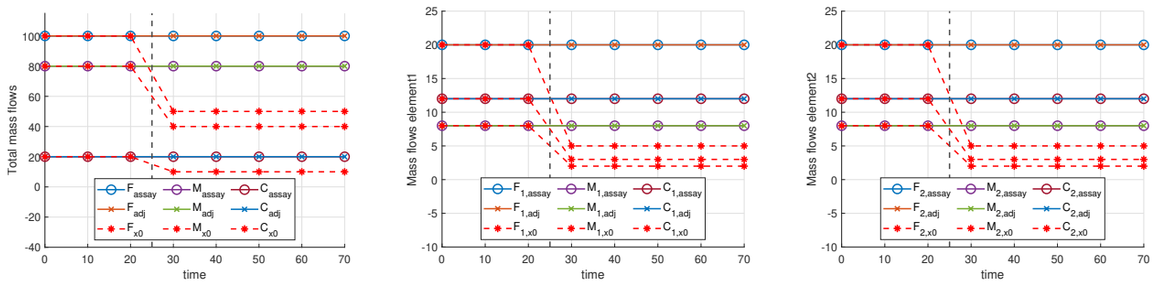

(a) Total mass flow (b) Mass flow element1 (c) Mass flow element2

Figure 12: *Assay and the adjusted values from optimization using "poor" initial guess. The values to the left of the dashed lines are fixed while the values to the right are adjustable. The dashed red line gives the initial guess.*

5.5.2 Optimization on Assay With Disturbances

To test the implementation further, one value of the assay was disturbed. Here the last sample of the feed was changed to $F(70) = 110$, a change equal to 10%. This causes the assay to no longer fulfill mass balance. The optimization took more than thirty minutes to complete and yielded the result shown in figure 13. The solution shows that the disturbed greatest relative adjustment of the values is done to the disturbed value. The disturbed value is adjusted, and the adjusted assay now resembles the undisturbed assay in figure 11, which fulfilled mass balance.

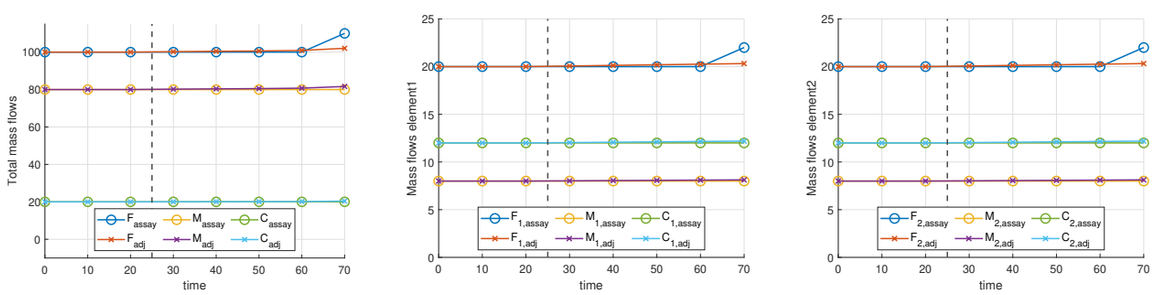

(a) Total mass flow (b) Mass flow element1 (c) Mass flow element2

Figure 13: *Assay and the adjusted values. The values to the left of the dashed lines are fixed while the values to the right are adjustable. The measurement of the total mass flow in the feed $F(70)$ causes the assay to not fulfill mass balance. The assay is adjusted such that the it fulfills mass balance.*

The same result is acquired for the case where a grade is disturbed. The grade of element2 is disturbed, changed to $c_2(60) = 0.66$ which is a change equal to 10%. The optimization took more than thirty minutes to complete and yielded the result shown in figure 14. The grade $c_2(60)$ was subjected to the greatest adjustment such that the adjusted assay fulfills mass balance.

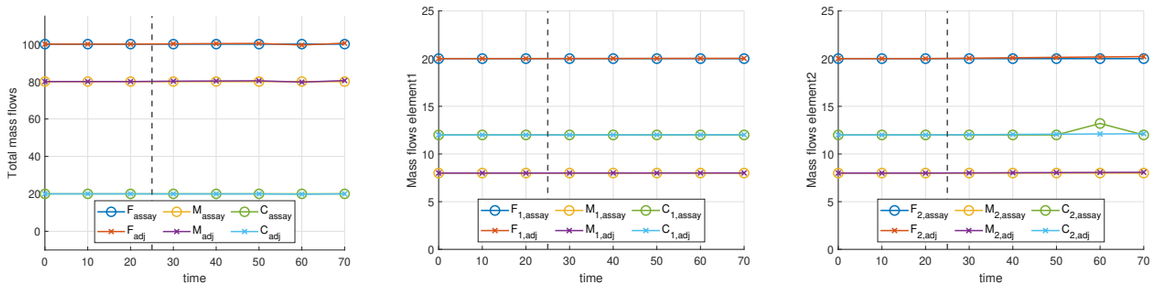

(a) Total mass flow (b) Mass flow element1 (c) Mass flow element2

Figure 14: *Assay and the adjusted values. The values to the left of the dashed lines are fixed while the values to the right are adjustable. The measurement of the grade in the concentrate* $c_2(60)$ *causes the assay to not fulfill mass balance. The assay is adjusted such that the it fulfills mass balance.*

5.6 Recovery by Fixpoint Iteration

The recovery of the flotation cell is is required by this model, but it is initially unknown. An attempt was made to determine the recovery of the flotation cell iteratively. The concept was that an initial guess of the recovery R_0 could be used to adjust the assay. The resulting assay would supply the adjusted feed $F_{\alpha,1}(t)$ and adjusted concentrate $C_{\alpha,1}(t)$. With these values, a new guess for the recovery, R_1, can be evaluated, and can in turn be used to adjust the assay. Eventually, the difference $|R_{i+1} - R_i|$ becomes sufficiently small and an optimal recovery has been found. However, there is a problem. The constraints enforces $C_{\alpha,i}(t)/F_{\alpha,i}(t) = R_i$, and thus $|R_{i+1} - R_i| = 0$ is always true. Since the recovery is crucial for this model, it must be found some other way.

6 Discussion

The desire to develop a formulation of unsteady-state mass balance for is hardly new and there are a number of approaches. Bazin and Franklin (1995) refer to three categories of handling real-time mass balance. The first category consider that there is no accumulation of mass in the circuit at time t and steady state is assumed while carrying out mass balance calculations using the most recent assay. The second category comes from assuming steady state over small windows in time and the values are averaged over this window. The third category is to use a process model to account for accumulation within the circuit [13]. Hence, the new model that is developed of this report belongs to the third category.

It is clear that dynamic models, the third category of on-line mass balancing models, have an advantage over window averaging models, the second category. Hodouin and Makni [14] proposed a method using filtering of measurements to dynamically reconcile flow rates and compositions of a complex mineral processing sheet. There were two models considered, one using steady-state nodes and the other using dynamic equations for the streams. The dynamic model significantly improved the data reconciliation procedure, since phase lags between true and filtered values that arose with window averaging procedures were avoided.

The strength of this model is the prediction of residence time in flotation series. In previous work accumulation delay is often regarded as static and the equal for each of the balanced elements. Here, not only is the delay related to the internal mass of the elements over time, but each element is also considered separately. This gives an advantage over methods that does not model this behaviour. Furthermore, the physical model of the delay is related to the nature of the buffer. Usually, the residence time of a series is approximated assuming either that a series of tanks is similar to one large tank or that the RTD for the series approaches plug flow. The ability to model how each tank contributes to the series' transfer of material allows for a more accurate description of the material transfer.

The results from the implementation of the model shows that the implementation does in fact optimize the assay by enforcing the constraints of mass balance. The solution is stable and does not stray from the initial assay if it fulfills mass balance. When an assay does not fulfill mass balance, the implementation performs the greatest adjustment to the "disturbed" value. Adjustments are done as expected regardless if there are disturbances in the mass flows or in the grades. Overall, the model seems to perform quite well for the single cell tests performed here. However, all tests here assume that the recovery, grades, and mass flows are constant, meaning that $\frac{dW_\alpha(t)}{dt} = 0$. More rigorous tests would include some change in the mass flow or grades in order to truly test the viability of this model. The advantage of the synthetic data used here was that it was quite simple to ensure that a mass balanced solution exists, which would also have to be confirmed for tests where $\frac{dW_\alpha(t)}{dt} \neq 0$.

The implementation of the optimization problem of mass balancing the mass flows and grades for a single cell with two elements took around thirty minutes. The measurements of mass flows and grades in the circuit are sampled roughly every fifteen minutes. This sets an upper bound on computation time if this method is applied for on-line mass balancing. If the mass balance takes longer than fifteen minutes, the optimization will gradually fall behind and nothing can be predicted. Thus, the implementation must be developed further in order to increase the speed of optimization.

It was found that one of the major time consuming parts of the implementation is the numerical double integration using `integral2`. This calculation is performed $2 \times N_j \times N_{\text{buffers}} \times N_{element}$. Since the computation time will only increase with the addition of buffers, elements, and enforced constraints, as more calls will be made to `integral2`, it is a prime point of improvement for the implementation. The computation for function `integral2` can be made shorter by adjusting the relative and absolute tolerances. These values determine the required accuracy of `integral2` and should reflect the expected errors of the grades and mass flows such that the requirement of accuracy is not unnecessarily strict. However, it is crucial that the sampling in time has higher resolution than the measurements. If simply the times of the measurements are used, then the dynamics of the transfer will not be captured and the solution will be of poor accuracy. Thus, this accuracy is a trade off in computation time and the tolerances must be strict enough to capture the dynamics in the model and lax enough as to not take unnecessary long time.

Since integrating the constraints takes a long time, solving the integrals once and reusing them provides a great opportunity to achieve shorter computation times. Since the integrals in the constraints only contain known functions, these can be calculated once and be replaced by numbers. Coincidentally, these integrals form the elements of the non-linear constraint Hessian, $\mathbb{H}_j$. Thus, the Hessian can be used to construct the constraints by vector-matrix-vector multiplication, $\mathbf{x}\mathbb{H}_j\mathbf{x}$ where $\mathbb{H}_j$ is the Hessian related to constraint j. However, there was a difference between numerically integrating each element independently compared to summing each element and then integrating. The difference was likely due to small numerical errors. This both increased the computation time for the numerical integration and reduced the accuracy for the method. The numerical errors could be explained by the discontinuities 'disappearing' when added onto a large integration, rather than integrating every part individually. Still, one can save a lot of time by evaluating the integrals once, even though the integrals are quite numerically heavy.

An attempt of using the Hessian to construct the constraints was made. Ultimately, this was not successfully implemented due to poorly conditioned matrices when the optimization function `fmincon` computed the steps for the solver. More testing is required to find the reason behind this poor conditioning and if the gradient of the constraints can be supplied in order to help the calculation of steps for the solver.

It has been stated that it is important to clearly separate the degrees of freedom from the variables in the mathematical formulation when implementing the constraints. The degrees of freedom in $\mathbf{x}$ are used to evaluate the constraints, but there are corresponding values for times $t < t_0$ that are not degrees of freedom. These values are the must be taken from some previous optimization or measured values. In this report, they have been referred to as the "accepted history". The reason for this name is that these values have in some way been tested enough that the expected error of these measurements is sufficiently small such that they

can be trusted to be as close to the true values as possible. Realistically, if there have several subsequent optimizations and the value of a specific measurement has been barely adjusted, it should become accepted as the true value. The contribution from the history dies off exponentially with time due to the RTDs and when the contribution from these historical values is considered sufficiently small then it can be truncated.

In this report, the constraint for the total mass flow states that the inflow into a cell is equal to to the outflow at every point in time, i.e. that the total outflow will change correspondingly to any change in the inflow. The reasoning behind this simplification was that there are level sensors used that automatically changes the outflow accordingly. Hence, the volume in each cell is constant and kept by constant adjustments in inflow and outflow. However, no two ores are the other alike, and the overall density of the slurry varies with time. The mass flows used in the mass balances are the so called *dry* mass flows meaning that the mass of the water in the slurry is not included in calculations. The assumptions that the change of the total mass inflow is immediately adjusted for in the outflow is clearly not true. To develop this model further is to add a term $\frac{dW(t)}{dt}$ to the total mass flow constraint, similarly to how the grade constraint involved delay.

The verification part in this report uses synthetic data to test the correctness of the implementation of the optimization problem that performs mass balancing of the sampled measurements. The synthetic data is obviously obviously a manufactured test case, but it is representative for the effectiveness of the optimization algorithm. To verify the models for the delay, this must be implemented with natural data. E.g. section 3.6 suggests how the cell specific parameter flotation rate k can be modeled. It is known to depend on the machine producing the bubbles in the flotation tank, the size and properties of the particles in the pulp in the tank, as well as the properties of the froth. The only way to verify the validity this model of k is to acquire natural data of material transfer from a real flotation circuit.

The transfer of material through a flotation tank is usually measured with either tracer test or batch flotations. Tracer tests, mentioned in section 2.2, usually involve the measurement of some radioactive material going in and then retrieved at the other end. However, since there are two outflows in in a flotation cell and the radioactive material does not necessarily take the same path as the element of interest, the radioactive material can not be taken as representative of the element of interest. On the other hand, batch flotations are done by taking a flotation cell that contains no material, other than water of course, and then an impulse is introduced in the system. However, since the flow in the system is not continuous, it is a batch flotation, the comparison model of a dynamic formulation for mass balance is unrealistic. Because neither of these tests would produce numbers to accurate natural data, the most intuitive approach to determine its accuracy is simply implementing the model directly.

Finally, since the recovery cannot be determined iteratively using this method, another strategy must be employed. A possible solution would be to re-formulate the current formulation such that the recovery is adjusted as well. The current formulation of the optimization problem is almost purely quadratic and somewhat simple to formulate. A reformulation including the recovery would likely be more complicated than the current formulation. Another possible solution would be to formulate an outer optimization problem. That way the recovery would be adjusted such that the minimized objective function of the inner optimization problem is minimized with respect to the residual as well. The recovery that minimizes the residual should be the true recovery. The second approach may be simpler to implement but there is further investigation needed to determine which of these would be optimal.

7 Conclusion

The verification of the method shows that the mass balancing gives feasible results for the synthetic data, which is representative for the model's behaviour on natural data. Thus, it is feasible that this model can provide on-line mass balancing and reconciliation of mass flows and grades in a flotation circuit. However, there is a lot to consider before this model can be implemented in a real circuit.

Due to time restrictions there were only a few tests that could be performed and an obvious next step is to perform further verification using synthetic data. Further verification should investigate the optimal algorithm and set-up of the problem to ensure sufficient computation speed. The upper limit for the mass balancing time is the sampling time, currently around every fifteen minutes. There are some choices in implementation that could severely reduce the computation times, such as using the Hessian of the non-linear constraints to construct the grade constraints. Optimizing algorithms similar to the `fmincon`'s 'interior-point' algorithm can also be supplied with the Hessian such that it does not have to use finite differences to find the next step for the solver [9]. Note that the structure of the problem might cause the matrices to become poorly conditioned, causing trouble for the solver when evaluating the steps.

The recovery is needed in this model, but the recovery is an unknown cell specific parameter. An iterative method to determine the recovery was attempted but did not work. There are two other possible solutions: either the current optimization problem is re-formulated such that the optimization problem includes the recovery, or an outer optimization problem for the recovery is formulated such that the residual of the inner optimization problem is minimized with respect to the recovery. Further investigation is needed to determine the superior strategy of determining the recovery. Regardless, the lack of known recovery must be addressed.

If the model has been implemented such that it is sufficiently fast and such that the recovery can be determined, this model may be implemented using natural data acquired from a flotation plant. This would give further insight of the limitations of the model. A model for the flotation rate k is described in section 3.6 but requires natural data since there is no way to prove its validity using synthetic data. Testing using natural data would allow to verify the validity of transfer functions and determine the requirements of accuracy. Since there are complications with performing tracer tests and batch flow tests, the best possible course of action would be to analyze and compare the adjustments made by a direct implementation on a flotation circuit.

The development of on-line mass balancing and reconciliation is on-going and has been for a while, including model-based and AI solutions, and it has proven to be challenging to develop reliable methods for mineral processing control [3]. This project shows a lot of promise for future mineral processing. Further development of this method could provide a method for on-line mass balancing and reconciliation which could in turn reduce losses to the tailings and allow for fast intervention of process failures, which in turn is extremely valuable for the mining industry.

References

[1] B. A. Wills and J. A. Finch, *Wills' Mineral Processing Technology: An Introduction to the Practical Aspects of Ore Treatment and Mineral Recovery*. Oxford, UK ; Waltham, MA: Butterworth-Heinemann, eigth edition ed., 2016.

[2] W. Rogers, M. Kahraman, F. Drews, K. Powell, J. Haight, Y. Wang, K. Baxla, and M. Sobalkar, "Automation in the mining industry: Review of technology, systems, human factors, and political risk," *Mining, Metallurgy & Exploration*, vol. 36, 06 2019.

[3] D. Hodouin, S.-L. Jämsä-Jounela, M. Carvalho, and L. Bergh, "State of the art and challenges in mineral processing control," *Control Engineering Practice*, vol. 9, no. 9, pp. 995–1005, 2001. Review Papers on Automation in Mineral and Metal Processing.

[4] NEW Boliden, "Års- och hållbarhetsredovisning 2020," Stockholm, 2020.

[5] G. Folland, *Fourier Analysis and Its Applications*. Advanced Mathematics Series, Wadsworth & Brooks/Cole Advanced Books & Software, 1992.

[6] M. G. Larson and F. Bengzon, *The Finite Element Method : Theory, Implementation, and Applications*. Heidelberg: Springer, 2013.

[7] C. Steyn and C. Sandrock, "Causal Model of an Industrial Platinum Flotation Circuit," *Control Engineering Practice*, vol. 109, 2021.

[8] I. The MathWorks, "Create a simple class." https://se.mathworks.com/help/matlab/matlab_oop/create-a-simple-class.html. Accessed: 2021-05-22.

[9] I. The MathWorks, "fmincon." https://se.mathworks.com/help/optim/ug/fmincon.html. Accessed: 2021-05-22.

[10] I. The MathWorks, "fmincon interior-point algorithm." https://se.mathworks.com/help/optim/ug/constrained-nonlinear-optimization-algorithms.html#brnpd5f. Accessed: 2021-05-22.

[11] I. The MathWorks, "integral." https://se.mathworks.com/help/matlab/ref/integral.html. Accessed: 2021-05-22.

[12] I. The MathWorks, "integral2." https://se.mathworks.com/help/matlab/ref/integral2.html. Accessed: 2021-05-22.

[13] C. Bazin and M. Franklin, "Real-time material balance for flotation plants using a least-squares recursive algorithm," *International Journal of Mineral Processing*, vol. Vol.46 (3), 1995.

[14] D. Hodouin and S. Makni, "Real-time reconciliation of mineral processing plant data using bilinear material balance equations coupled to empirical dynamic models," *International Journal of Mineral Processing*, vol. Vol.48 (3), 1996.

A Glossary

English	Swedish	Description
Assay	Mätserie	A set of samples over a circuits products and buffer.
Cleaner	Repetering	A secondary series of flotation tanks that subsequent to the raw series concentrate. The purpose of this series is to achieve an even higher concentration of pay mineral.
Comminution	Pulverisering	The act of finely crushing ore into particles that consist of a single element.
Concentrate	Koncentrat	Portion of the mineral processing that is enriched with pay mineral.
Convolution	Faltning	Mathematical operation that constructs a new integrable function out of two integrable functions.
Flotation	Flotation	A concentrating method used in mineral processing that exploits the surface properties of the material in the slurry. The valuable mineral is made hydrophobic and the less valuable material is made hydrophilic. Bubbles of air are introduce such that the hydrophobic valuable mineral can attach to them, floating to the top of the slurry.
Flotation Series/- Block/ - Bank	Flotationsserie/-block/-bank	A number of flotation tanks placed in sequence.
Flotation Tank/- Cell	Flotationstank/-cell	A container where the flotation process takes place. An illustration is shown in figure 1.
Froth	Skum	A mass of small bubbles in liquid caused by agitation.
Froth Recovery	Skumutbyte	The amount of pay mineral that was in the froth that goes to the concentrate and does not drop back to the slurry.
Gangue	Gråberg	The non-marketable material found in ore.
Grade	Halt	The amount of mineral in any stream of material.
Ore	Malm	A deposit of greater concentration of minerals.
Pay Mineral	Värdemineral	The marketable mineral that resides in the ore.
Reconciliation	Haltjustering	The act of adjusting values such that they are compatible.
Recovery	Utbyte	The percentage of pay mineral that was entered via the feed that was found in the concentrate.
Residence Time	Uppehållstid	The amount of time it takes for a fluid element to transfer through a control volume.
Scavenger	Scavenger	A secondary series of flotation tanks that is subsequent of the raw series tail. The purpose of this series is to retrieve the most out of the losses to the tail.
Slurry/pulp	Slurry/Pulp	A mixture of water and finely ground ore.
Tail	(Slut-) Mellanprodukt	Portion of the mineral processing that contains almost no pay mineral and is generally discarded or scavenged.